Title
Cervical Epidural Electrical Stimulation Activation of Spinal Respiratory Sensorimotor Circuits

Author
Galer, Erika

Publication Date
2021

Peer reviewed|Thesis/dissertation

UNIVERSITY OF CALIFORNIA

Los Angeles

Cervical Epidural Electrical Stimulation Activation of Spinal Respiratory Sensorimotor Circuits

A dissertation submitted in partial satisfaction of the requirements for the degree of Doctor of Philosophy in Molecular Cellular and Integrative Physiology

by

Erika Lane Galer

2021

ABSTRACT OF THE THESIS

Cervical Epidural Electrical Stimulation of Spinal Sensorimotor Respiratory Circuits

by

Erika Lane Galer
Doctor of Philosophy in Molecular Cellular Integrative Physiology
University of California, Los Angeles, 2021
Professor Daniel Lu, Chair

Brainstem and spinal cord neurons generate patterned activity necessary for the execution of respiration. The spinal circuit integrates sensory, propriospinal, and supraspinal inputs with endogenous rhythmic neuronal activity to coordinate excitation of phrenic motor neurons and other muscles with respiratory-related activity. In Chapter 2, we tested the hypothesis that dorsal cervical epidural electrical stimulation (CEES) would increase respiratory activity in anesthetized rats. Respiratory frequency and minute volume were significantly increased when CEES was applied to the cervical spinal cord between C2 and C6. We injected pseudorabies virus into the diaphragm to label respiratory-related neurons in the spine and brainstem and elicited c-Fos activity during CEES. We identified neurons in the dorsal horn of the cervical spine in which c-Fos and pseudorabies were colocalized, and these neurons also expressed somatostatin (SST). Using dual viral transfection to express the inhibitory Designer Receptor Exclusively Activated by Designer Drugs (DREADD), hM4D(Gi), selectively in SST-positive cells, we were able to inhibit SST-expressing neurons by administration of Clozapine N-oxide (CNO). The respiratory excitation elicited by CEES was diminished in the presence of CNO. We conclude that dorsal cervical epidural stimulation activated SST-expressing neurons in the cervical spinal cord, likely interneurons that communicated with

more rostral elements of the respiratory pattern generating network to effect the changes in tidal volume and frequency that were observed.

Respiratory complications are a leading cause of morbidity and mortality following cervical spinal cord injury. Mechanical ventilation is the main intervention that itself carries negative side-effects. Novel forms of neuromodulation have been explored to enhance respiratory activity in the injured spinal cord; yet, are often difficult to clinically execute. In Chapter 3, we explored dorsal CEES to increase diaphragm activity in anesthetized rats that underwent a C2 hemisection causing respiratory deficits. CEES increased the probability of rhythmic bursting in the once paralyzed (ipsilateral) diaphragm. The activity observed was significantly increased compared to sham trials. We found increases in rhythmic diaphragm activity waned after stimulation ceased. These results demonstrate that dorsal CEES can enhance respiratory activity after high cervical spinal cord injury. Further exploration could lead to a novel therapy for respiratory deficits after spinal cord injury.

The dissertation of Erika L Galer is approved.

Marc R. Nuwer

Thomas J. O'Dell

Ronald M. Harper

Scott H. Chandler

James C. Leiter

Daniel C. Lu, Committee Chair

University of California, Los Angeles

2021

Contents

Figures and Tables

Acknowledgements

I would like to thank Dr. Lu and Dr. Leiter for their support throughout my graduate career. Thank you Dr. Lu, for providing a flexible environment that allowed space to learn that the pursuit of science and expanding knowledge includes a series of failures and mistakes. In addition, it is the work of learning from those mistakes and dedication to continually refine and expand questions that makes a good scientist. In your lab, I have become a confident scientist. Thank you for having faith in me when I questioned myself. Thank you Dr. Leiter, for taking the time to listen and work through the experimental and writing details. The guidance you have patiently provided me is appreciated. I aspire to wow others with my knowledge of respiratory physiology in so many animal species, as you have wowed me. It is the willingness you have demonstrated, spending your time (often after hours) teaching young scientists that keeps science true to its craft. And I feel confident moving forward knowing I have the lessons and tools you taught me. Together, you both have provided me an endless list of lessons and tools that I plan to use and continue to improve upon in my professional career, as well as in my personal life.

I would like to thank my parents for their endless support throughout the years. You both taught me the importance of hard-work and dedication to a goal until completion. I am able to take risks and pursue success because you have always believed I could. Your support has kept me moving forward and you inspire me to always be the best version of myself.

Thank you friends and collegues that have cried and cheered with me. Teamwork makes dreams happen.

Vita

Education

University of Colorado Boulder 2013

Boulder, CO

Bachelor of Arts in Psychology and Molecular Cellular and Developmental Biology

Publications

Publications in Preparation:

Galer EL, Moore LD, Zdunowski S, Zhong H, de Lucena DS, Duarte J, Norman SL, Reinkensmeyer DJ, Edgerton VR, Leiter JC, Lu DC. Epidural electrical stimulation of the spinal cord improves reaching accuracy following stroke injury of the forelimb cortex in rats. (in submission).

Galer EL, Madhaven M, Wang E, Huang R, Leiter JC, Lu DC. Cervical epidural electrical stimulation increases respiratory activity through somatostatin-expressing neurons in the dorsal cervical spine in rats. (in preparation).

Galer, EL, Madhaven MM, Mekonnen MM, Leiter JC, Lu DC. Cervical epidural electrical stimulation restores spontaneous coordinated respiratory activity in paralyzed anesthetized rats. (in preparation).

Huang R, Worrell J, Garner E, Wang S, Homsey T, Xu B, **Galer EL,** Tazakol S, Daneshvar M, Le T, vonTrotha N, Vinters HV, Salamon N, McArthur DL, Nuwer MR, Wu I, Leiter JC, Lu DC. Epidural electrical stimulation of the cervical spine reverses respiratory depression induced by opioid-induced respiratory depression. (in submission).

Peer-Reviewed Publications:

Grace PM, **Galer EL,** Strand KA, Corrigan K, Berkelhammer D, Maier SF, Watkins LR. *Repeated morphine prolongs postoperative pain in male rats.* Anesth Analg. 128(1):161-167 (2019).

Grace PM, Strand KA, **Galer EL**, Maier SF, Watkins LR. *MicroRNA-124 and microRNA-146a both attenuate persistent neuropathic pain induced by morphine in male rats.* Brain Res 1692:9-11 (2018).

Grace PM, Strand KA, **Galer EL**, Rice KC, Maier SF, Watkins LR. *Protraction of neuropathic pain by morphine is mediated by spinal damage associated molecular patterns (DAMPs) in male rats.* Brain Behav Immun 72:45-50 (2018).

Grace PM, Wang X, Strand KA, Baratta MV, Zhang Y, **Galer EL**, Ying H, Maier SF, Watkins LR. *DREADDed microglia in pain: Implications for spinal inflammatory signaling in male rats.* Exp Neurol 304:125-131 (2018).

Grace PM, Fabisiak TJ, Green-Fulgham SM, Anderson ND, Strand KA, Kwilasz AJ, **Galer EL**, Walker FR, Greenwood BN, Maier SF, Fleshner M, Watkins LR. *Prior voluntary wheel running attenuates neuropathic pain.* Pain 157(9):2012-2023. (2016).

Grace PM, Strand KA, **Galer EL**, Urban DJ, Wang X, Baratta MV, Fabisiak TJ, Anderson ND, Cheng K, Greene LI, Berkelhammer D, Zhang Y, Ellis AL, Yin HH, Campeau S, Rice KC, Roth BL, Maier SF, Watkins LR. *Morphine prolongs neuropathic pain via NLRP3.* Proceedings of the National Academy of Sciences, 113(24) E3441-E3450 (2016).

Galer, EL, & Grace, PM. *Reactive aldehydes: a new player in inflammatory pain*. Annals of Translational Medicine, 3(Suppl 1), S23 (2015).

Northcutt AL, Hutchinson MR, Wang X, Baratta MV, Hiranita T, Cochran TA, Pomrenze MB, **Galer EL**, Kopajtic TA, Li CM, Amat J, Larson G, Cooper DC, Huang Y, O'Neill CE, Yin H, Zahniser NR, Katz JL, Rice KC, Maier SF, Bachtell RK and Watkins LR. *DAT isn't all that: cocaine reward and reinforcement requires Toll Like Receptor 4 signaling*. Molecular Psychiatry, 20(12) 1525-1537 (2015).

Hutchinson MR, Northcutt AL, Hiranita T, Wang X, Lewis SS, Thomas J, van Steeg K, Kopajtic, TA, Loram LC, Sfregola C, **Galer E**, Miles NE, Bland ST, Amat J, Rozeske RR, Maslanik T, Chapman TR, Strand KA, Fleshner M, Bachtell RK, Somogyi AA, Yin H, Kats JL, Rice KC, Maier SF, and Watkins LR. *Opioid activation of toll-like receptor 4 contributes to drug reinforcement*. Journal of Neuroscience, 32(33): 11187-11200 (2012).

Chapter 1

Preface

Respiration is a vital behavior resulting in the exchange of oxygen and carbon dioxide to sustain metabolic processes in all organisms. It is an automatic process, continuing through all states of sleep and wakefulness. However, respiration is also a volitional behavior that contributes to somatic processes, such as airway clearance, vocal and non-vocal behaviors, physical activity, and emotional expression. Given the importance of these functions to sustaining life, research describing the neural circuits that maintain and modulate respiration must continue until our understanding is complete. Doing so will then speed progress in the research exploring novel therapies that improve respiratory function after disease and injury.

A variety of respiratory systems and patterns exist across species that change according to conditions in the environment, physiological states, and muscle activation. The information reviewed in this thesis will focus on adult human, primate, and small mammal respiratory systems and physiology. Chapter 1 explores the known respiratory muscles, neural circuits, and their interactions, as well as an introduction to advanced technologies used in research.

Introduction

The primary muscle of spontaneous, automatic breathing is the diaphragm. The diaphragm is innervated by the phrenic nerve, which projects from the ventral spinal cord at cervical levels 3-5 (C3-5)[1] [1-3]. During inspiration, the diaphragm contracts away from the lungs to increase the pleural cavity's volume, thereby lowering the pressure on the lungs. The drop in pressure allows air to fill the lungs [4]. The expiration that follows is passive during "eupnea", or calm, unlabored, breathing: the volume of the

[1] Variations of the cervical levels in which the phrenic motor neurons reside and its projections via the phrenic nerve exit the spinal cord exist among species.

pleural cavity decreases as the diaphragm relaxes, increasing pressure on the lungs. This pressure and the elastic recoil of the lungs expels air.

Active respiration, during activity or air way clearance, utilizes a broader set of muscles. In this condition, the scalene, sternomastoid, external intercostal, and pectoralis muscles expand the chest out to further increase pleural cavity volume. The internal intercostals and abdominal muscles work as pressure generators during active expiration to decrease the pleural cavity size, thereby pushing larger amounts of air from the lungs and acting on a quicker time scale. Precise coordination between the muscle groups of inspiration and expiration are important to maintain mechanics resulting in successful respiratory cycling. If the coordination is lost or if there is a loss of muscle activity, paradoxical movements of the chest and abdomen will occur causing respiratory deficiencies.

The behavior of eupneic respiration is divided into 3 phases: inspiratory (I), post-inspiratory (post-I), and expiratory (E) [5-7]. This behavior is generated by nuclei within the brainstem, which provide excitatory drive to establish respiratory rhythm and pattern generation [8-10]. In addition, inhibitory activity within and between the nuclei play an important role to maintain respiratory rhythm and pattern. The excitatory and inhibitory activity is supplied by sets of neurons firing prior to inspiration (pre-I), during inspiration (I), after inspiration (post-I), and during expiration (E). These neurons comprise circuits communicating among and between themselves to establish respiratory behavior. The respiratory nuclei and circuits have been studied in order to understand the neuronal underpinnings of respiratory activity. These experiments included neonatal brainstem slice preparations, perfused brainstem and spinal cord preparations, *en bloc* preparations, and *in vivo* experiments.

Respiratory Neuroanatomy and Physiology

The brainstem is a structure located at the base of the brain proper. It contains nuclei pertinent to many autonomic processes and fibers traveling from the brain to the spinal cord. In the portion of the brainstem known as the pons (Latin for “bridge”), the Kölliker-Fuse nucleus (KF) and the Parabrachial nucleus (PB) coordinate phase transition and respiratory rhythm [11-14]. Phase transition refers to the timing and

switch between inspiratory to expiratory behavior. In the medulla, the parafacial respiratory group (pFRG) and the retrotrapezoid nucleus (RTN) intersect and contain pre-I neurons which are genetically defined as Phox2B [9, 15, 16]. Some of these Phox2B neurons within the pFRG and RTN are inherently chemosensitive and provide input that modulates respiratory activity [17-20]. During these periods of enhanced neural drive (e.g., hypercapnia, hypoxia, exercise) neurons in the pFRG and RTN fire during the late expiratory period (late-E) and send input to the caudal ventral respiratory group (cVRG), which contain premotor neurons to accessory muscles for active expiration [21, 22].

Rostral to the cVRG is the Botzinger Complex (BotzC) and the Pre-Botzinger Complex (Pre-BotzC). The BotzC is a nucleus containing post-I and late-E neurons, which participate in the maintenance of the expiratory phase transition [23]. The BotzC monosynaptically inhibits phrenic motor neurons, providing a direct circuit to coordinate muscle activity during the expiratory phase [24]. The Pre-BotzC is a nucleus that contains a heterogeneous mix of pre-I and I-spanning interneurons projecting to the other known respiratory nuclei within the brainstem that, contribute to inspiratory rhythmogenesis [25-29]. Neurons in the Pre-BotzC have intrinsic bursting capabilities attributed to their expression of persistent Na+ channels and Ca^{2+}-activated cationic currents [25, 26, 30-35]. Together they keep the neurons at a higher resting membrane potential and maintain repeated rises beyond the action potential threshold to achieve rhythmic bursting without external influence. These ion channels have biophysical properties to activate and inactivate based on the membrane potential. This characteristic enables neuronal circuits to modify their activity to the dynamic needs of the system.

The rostral ventral respiratory group (rVRG) contains projections to the brainstem and the spinal cord. I-neurons in the rVRG project to brainstem nuclei that control upper airway muscles involved in respiratory activity as well as to aforementioned respiratory brainstem nuclei [36]. Phrenic premotor neurons in the rVRG project to the phrenic nucleus in the cervical spinal cord [23]. In some mammals such as rabbits, the dorsal respiratory group (DRG) within the medulla contains premotor neurons that project ipsilaterally to the cervical spinal cord onto phrenic motor neurons innervating the diaphragm [37, 38].

What other connections exist between these respiratory brainstem nuclei and the spinal cord? A theory or principle of neurophysiology suggests that redundancy among functional circuits commonly exists to mitigate deficits when a circuit is compromised. Therefore, we should consider whether redundant respiratory circuits exist in the spinal cord to mitigate brainstem injury or disease. There is evidence that I neurons exist in cervical spinal cord levels 1 and 2 (C1-C2) in cats and mice [39-41]. Upper cervical I neurons project to cervical, intercostal, and lumbar regions of the spinal cord with collateral projections to cervical regions [39, 40, 42]. These I neurons have antidromic action potentials in response to phrenic and intercostal peripheral nerve stimulation, suggesting direct connections between these neurons [39, 40, 42]. Furthermore, the upper cervical respiratory neurons receive projections from the respiratory brainstem nuclei discussed above [43].

These findings suggest that upper cervical respiratory neurons receive and project excitatory drive to spinal respiratory motoneurons. In fact, spontaneous and pharmacologically-induced phrenic nerve activity has been observed in the absence of supraspinal input altogether [44-47], such as when rhythmic bursting, arrhythmic bursting, and tonic phrenic nerve activity were recorded after complete cervical transection in rats, cats, and rabbits [46-48]. In cats, spontaneous rhythmic phrenic nerve activity was observed several hours after a complete spinal transection at C1 but not observed after C3 transection [46]. These results further suggest that upper cervical respiratory neurons play a role in rhythmic respiratory input. Yet there is little evidence of endogenous phrenic nerve activity in the absence of supraspinal input having a sustainable influence on continuous rhythmic respiratory activity.

Such is the current understanding of respiratory nuclei and interneuronal circuits. Much of this work relied upon experimental techniques that isolate specific nuclei, such as *in vitro* brainstem slice preparations, *in vitro* brainstem and spinal cord preparations, decerebrate preparations, and *in vivo* experiments. These preparations often necessitate experimental conditions atypical of most physiological states. Sometimes they rely upon nerve activity from respiratory accessory nerves but not activity which is specific to the phrenic nerve. And the observed rates of respiratory activity are often much slower than

what is observed *in vivo*. A more integrated review of respiratory rhythmogenesis suggests that the intrinsic bursting capabilities of all the brainstem and spinal cord respiratory nuclei contribute to rhythmic drive [49, 50]. In addition, the spinal cord plays an integral role in shaping the descending information in order to activate muscles for the physiological needs of the organism [51-53].

Spinal Cord Neuroanatomy and Respiratory Circuits

The spinal cord is a large bundle of neuronal fibers that is systematically structured to incorporate input from supraspinal structures with the continuous feedback about the state of the system from the periphery that allows for quick, adaptive modifications to a circuit (Figure 1). Many circuits of inhibitory and excitatory neurons exist within the spinal cord that coordinate muscles along the body's axis during important behaviors such as running; transitions from walking to running; coordinating respiratory rhythm with locomotion speed; respiratory depth and frequency modulation for O_2 and CO_2 homeostasis; exhaling; and core stability [54-58].

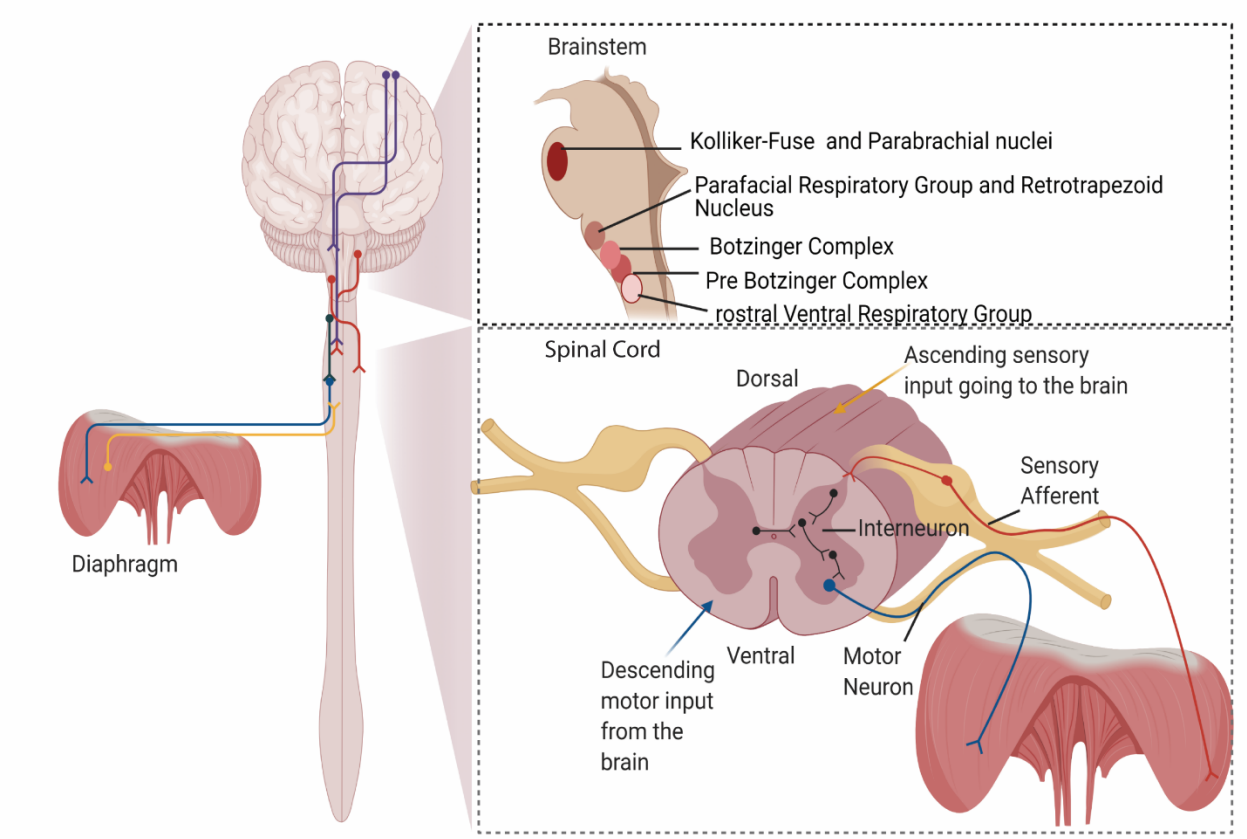

Figure 1.1: Neural anatomy of known respiratory nuclei and circuitry. Lying at the base of the brain, the brainstem has known nuclei that together generate rhythmic neuronal activity and send excitatory pre-motor projections (from rostral Ventral Respiratory Group (rVRG)) to the cervical spinal cord to initiate rhythmic diaphragm activity for respiratory behavior. The nuclei in the brainstem together generate and coordinate timing of respiratory behavior. Pre-motor connections from the rVRG descend and project ipsilateral and contralateral to their cell body and monosynaptically innervate phrenic motor neurons that project to the diaphragm muscle. The spinal cord is intricately formed in such a way that similar information systems are grouped into the dorsal and ventral aspects of the cord. Afferent cells and projections to the brain are on the dorsal part of the cord while efferent cells and projections to the spinal cord are on the ventral part of the cord. Motor neurons innervating the diaphragm (as well as the other accessory respiratory muscles) are in the phrenic nucleus of the spinal cord (C3-C5). Sensory afferents relay information from the muscles and dermis to the spinal cord and brain. Excitatory and inhibitory interneurons within the spinal cord modulate existing supraspinal input to the needs of the system by integrating the sensory and supraspinal input. Made using BioRender.com.

Motor neurons within the ventral spinal cord project to muscles of the periphery and precipitate muscle contraction. Interneurons (neurons with local spinal projections) and propriospinal neurons (neurons that project along the rostral-caudal axis of the spinal cord) are responsible for the coordination of muscles and the modulation of supraspinal input [40, 50, 59, 60]. Respiratory inter- and propriospinal neurons have been studied in a variety of species; they are located in the dorsal, central, and ventral regions of the cervical, thoracic, and lumbar spinal cord [59-62]. Inter- and propriospinal neurons have either inhibitory

or excitatory effects on the circuit it influences. These neurons fire action potentials at different phases of the respiratory cycle and receive antidromic action potentials from phrenic and intercostal nerve stimulation [63-66]. rVRG phrenic premotor projections directly synapse on spinal interneurons [67]. Thus, interneurons and propriospinal neurons are an integral part of a physiologically-in-tact respiratory system.

Muscle and system feedback are essential components of the spinal interneuron modulation of respiratory activity. Chemosensory neurons, located peripherally in the carotid bodies and centrally in the pFRG and RTN, actively sense $H+/CO_2$ fluctuations to provide feedback for systemic changes to respiratory activity in order to maintain homeostasis [68, 69].

Sensory afferents, which have projections from the muscle and tissue to the spinal cord, are integral to modulating supraspinal input as well as coordinating and executing rapid neuronal activity such as reflexes [70]. Sensory afferents are categorized on a number system and differ in size, architecture, receptor expression, and myelination (a factor that determines conduction velocity). These differences, as well as the location and architecture of their dendrites determine the type of sensory information they encode. Muscle spindles and golgi tendon organs (Type I) respond to muscle stretch and tension; they are large and thickly-myelinated to make their conduction velocities low. Mechanoreceptors (Type II) respond to and encode information on the pressure and position of muscles. Thinly-myelinated (Type III) and non-myelinated (Type IV) sensory afferents are small with a lower activation threshold and respond to temperature, pain, touch, and pressure.

Diaphragm sensory afferents provide dynamic feedback to spinal interneurons that polysynaptically modulate phrenic motor neuron activity [71, 72]. The diaphragm expresses fewer Type I and II sensory afferents compared to other muscles [72]. A majority of the sensory neurons that project from the diaphragm are Type III and IV afferents which increase respiratory activity [72]. It is likely that this increase is achieved through activity in a polysynaptic circuit because there exists no evidence of

monosynaptic activation of phrenic motor neurons from phrenic afferents [71, 73, 74]. Furthermore, afferents project to interneurons within the spinal cord that synapse on neurons relaying signals to the thalamus, primary sensory cortex, and brainstem [72, 75, 76]. These areas are known to modulate respiratory activity [72, 75, 76].

Research Techniques

Advances in research techniques have been integral to the understanding of isolated neural circuits and their effects on physiological systems and behavior. One technique uses viral hosts to access neuronal DNA, whereafter exogenous proteins are expressed in neurons which can then be used to activate or inhibit the neuronal output. Often these experiments use the bacterial Cre recombinase (a protein that serves to initiate DNA recombination events) and LoxP sites (DNA sequences to which Cre binds in order to recombine DNA sequences) (Figure 2) [77, 78]. Changes to LoxP sequences allow for excision, insertion, or restructuring of DNA sequences.

In order to modulate specific neuronal types, genetically modified animals have been created that express Cre downstream of specific promoters (sequences in the DNA that define the start of transcription of a gene to be expressed in a cell) and are commonplace in research laboratories. These animals can be used to express exogenous proteins in specific neuronal subsets when a viral vector is inserted that contains both the DNA material of the protein to be expressed and the LoxP sites. Opsins (light-gated ion channels) and Designer Receptor Exclusively Activated by Designer Drugs (DREADDs), are common exogenous proteins expressed in subsets of neurons (Figure 2). Within each of these types of proteins, differences exist that result in either activation or inhibition of the neuron in which it is expressed. For example, Channelrhodopsin 2 (ChR2), an opsin found in microbial eukaryotes, serves as a cation channel to depolarize the membrane potential in response to light [79]. Thus, when it is expressed in glutamatergic neurons in the cervical spinal cord, it is possible to trigger phrenic nerve activity after a complete C1 transection by exposing the spinal cord to light [79, 80]. Similarly, glutamatergic interneurons in the spinal cord can be activated with expression of hM3Dq, a DREADD that activates a cascade of protein

interactions resulting in Ca^{2+} increase and neuronal activation [81, 82]. The glutamatergic interneuron activation initiates phrenic motor neuron activity in the absence of supraspinal input [65, 81]. In the adult nervous system, glutamatergic neurons have an excitatory action on post-synaptic neurons. Thus, excitatory interneuron activity can sustain rhythmic phrenic nerve activity in the absence of the dominant bulbospinal circuit. The use of genetically modified animals with exogenous protein expression has provided researchers with improved ways of isolating neuronal circuits, resulting in evidence of an excitatory interneuron population that can provide rhythmic excitatory drive to phrenic motor neurons.

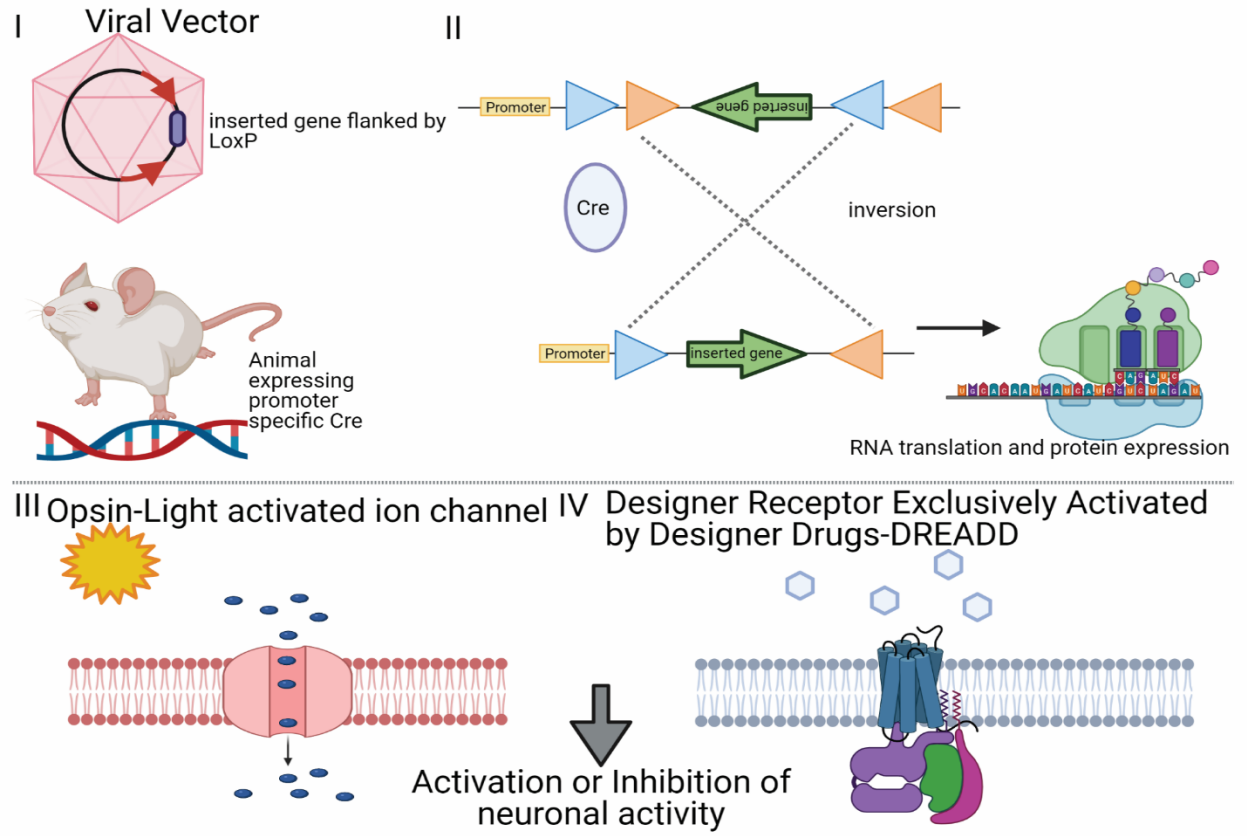

Figure 1.2: Advances in research tools have allowed for changes to neuronal activity in a population specific manner. Using viral expression of Cre recobinase and the necessary LoxP sites for it to bind, expression of exogenous proteins that alter the activity of the cell has become useful to neuroscientists looking to understand a specific population of cells dependent on the cells expression of other proteins. That is, Cre expression downstream of endogenous DNA promoters and the exogenous protein to be expressed between LoxP sites results in opsins or Designer Receptor Exclusively Activated by Designer Drugs (DREADD) being expressed in cells dependent upon their expression a specific endogenous protein. Optogenetics uses expression of light-gated ion channels. DREADDs uses expression of g-protein coupled receptors. The activation of the exogenous proteins results in activation or inhibition of the neuron it is being expressed in. Made with BioRender.com

Pharmacological agents are also extensively used to investigate neuronal circuits. The above experiments were conditional upon the presence of GABA/Glycine antagonist which inhibit GABA/Glycine activity. GABA/Glycine have an inhibitory affect in the adult central nervous system. GABA-mediated inhibition of phrenic nerve activity occurs during the expiratory phase and can be utilized to modify inspiratory activity [83, 84]. Inhibition of cervical spinal cord inhibitory activity leads to phrenic motor neuron activity in the absence of rVRG projections to phrenic motor neurons [85]. Together these experiments show excitatory and inhibitory interneuronal circuits within the spinal cord play a prominent role in shaping respiratory behavior. The use of pharmacological agents with known effects help scientists explore these circuit dynamics and can lead to the development of approved pharmaceuticals for use in human conditions.

So far, respiration, respiratory muscles, and the neural structures which contribute to respiration have been reviewed. Additionally, the contribution of technical and biomedical advances in research to understanding spinal circuitry controlling and modifying rhythmic muscle activity has been discussed. The following chapters present experiments undertaken to expand our understanding of the cervical spinal respiratory circuit and explores a novel therapeutic approach for respiratory-compromising conditions.

Chapter 2

Introduction

Since respiration and its related behaviors are essential components to life, research advancing our understanding and methods of modulation are important for improved health outcomes. Currently, positive pressure mechanical ventilation is the main therapy used in cases of respiratory dysfunction. Yet, use of positive pressure mechanical ventilation has negative side-effects such as diaphragm atrophy, lung damage, and higher incidence of pneumonia.

The brainstem nuclei, discussed in Chapter 1, maintain respiratory activity. Yet, these centers are difficult to access surgically and complications would be devastating. Circuits within the spinal cord contribute to respiratory behavior and current technologies exist that activate spinal sensorimotor circuits. Epidural electrical stimulation (EES) of the spinal cord is currently an FDA-approved therapy for chronic pain [86-88]. It has also been used to enhance descending circuits from the brain [89, 90]. And in research to probe spinal circuits involved in the rhythmic activation of muscles for locomotion in the lumbar spinal cord [91].

EES applied to the dorsal cervical spinal cord increases ventilation in anesthetized mice [92]. To expand this observation to another research species, the following set of experiments investigated cervical EES (CEES) modulation of respiratory activity and neuronal activation in anesthetized rats. After establishing ventilation increases during CEES in rats, we explored neuronal activation in respiratory transsynaptic labeled spinal interneurons, using the early expression protein c-Fos and pseudorabies virus (PRV-152). A subset of neurons expressed c-Fos and PRV in the dorsal horn. Since somatostatin expression is a known descriptor of brainstem neurons important to the maintenance of rhythmic respiration, we explored SST expression co-localized with the activated interneurons (labeled with c-Fos and PRV). [29]. SST was observed co-localized with c-Fos and PRV. We next investigated cervical SST neuronal activation involvement in CEES-induced respiratory activity using chemogenetic techniques. Using hM4Dgi (a

DREADD) to inhibit SST-expressing neuronal activity, we show CEES-induced ventilatory increases involve cervical SST interneuron activation.

Materials and Methods

Mixed-gender Sprague-Dawley rats (250-350 g, n = 49) were purchased from Envigo and allowed to acclimate in the UCLA vivarium for one week. Animals were kept in 12-12 light-dark cycle with *ad libitum* access to standard food and water. All procedures were approved by the University of California Animal Research Committee (protocol # 2014-122) and were conducted in accordance with the Guide for the Care and Use of Laboratory Animals of the National Institutes of Health.

Pseudorabies virus polysynaptic retrograde tracing and epidural electrical stimulation at C2/3 induced c-Fos activation

The Bartha strain of pseudorabies virus (PRV-152), supplied by the Center for Neuroanatomy with Neurotropic Viruses, NIH Virus Center P40 OD010996), was injected into the diaphragm of animals to label spinal respiratory neurons. Animals (n = 12) were anesthetized with isoflurane and a horizontal abdominal incision was performed to expose the diaphragm. Four 10 uL injections of 9 x 10^8 pfu/mL of PRV-152 were made bilaterally into the diaphragm using a Hamilton syringe and 30 g needle [67]. The abdominal tissue was closed with 5-0 Vicryl, and the skin incision was closed with staples. Animals were housed in a biohazard vivarium for 60 hours, after which they were transported to the lab and prepped for EES experiments.

Epidural electrical stimulation at C2/3 in PRV-152-expressing rats and c-Fos activation

The CEES studies were conducted 64-66 hours after PRV injections in each animal. This interval between PRV injection and EES allowed sufficient time for polysynaptic labeling of premotor neurons and putative spinal respiratory interneurons [67, 93]. During each CEES experiment, the rat was kept on a water-circulating heating pad to prevent hypothermia during the experiment. Animals were anesthetized with urethane (1200 mg/kg) and alpha-chloralose (30 mg/kg). A vertical incision was made ventrally on the neck; the sternohyoid muscles were separated to expose the trachea; a small incision was made between the

cartilage rings of the trachea; a short segment of PE 200 tubing was inserted to tracheostomize each animal; and the tracheostomy tube was connected to a pneumotach (Validyne, Northridge, CA) to record respiratory airflow. Two wires (St. Steel 7 Strand, AM-Systems, Sequim, WA), with the insulation stripped at the end (2 mm), were inserted bilaterally through abdominal incisions into the lateral costal portion of the diaphragm muscle to record electromyographic (EMG) activity. Each animal was flipped prone and a laminectomy was performed to expose C2-C7 spinal cord levels. Dorsal CEES was performed using a stimulating electrode (Tungsten Parylene 0.01, AM-Systems) placed ~2 mm lateral to the midline on the dorsal surface of the cervical spine, and the ground electrode was placed on the dorsal surface of the spine ~2-3 mm away from the stimulating electrode. The ends of the electrodes were stripped, leaving ~2 mm of the electrode tip uninsulated. CEES was delivered as a continuous 30 Hz monophasic (500 μs pulse width) train of impulses for 30 s (Master 9 A.M.P.I., Jerusalem, ISR). EMG signals were amplified x 1000, bandpass filter at 300-1000 Hz, and a 60 Hz Notch filter applied. Diaphragmatic EMG activity was sampled throughout each study at a rate of 2 kHz.

Animals were randomized to receive six trials of 30 second active CEES (n = 9) and sham stimulation or sham (n = 3) stimulation only at the intersection of cervical levels 2 and 3 (C2/3). Sham stimulation trials in the CEES group were performed to control for any effects that the electrode pressure on the dura may have had on respiration behavior in the absence of current. Experiments in which animals received only sham stimulation were performed to control for c-Fos expression in the unstimulated condition. To execute the sham trials, the stimulation and ground electrodes were placed on the dura with similar pressure as stimulation trials, but no stimulation was delivered. During sham stimulation (Sham) and active stimulation trials (Stim) data were recorded for 1 min of baseline recording, 30 sec Stim/Sham, and 8-10 minutes post-Stim/Sham. Data presented are the 30 sec prior to Stim/Sham (Pre), 30 sec of Stim/Sham (Intra), and 30 sec of post Stim/Sham (Post). Each animal was allowed to survive for at least one hour past the mid-way point of stimulation to allow c-Fos expression to develop.

Visualization of PRV-152, c-Fos, and somatostatin

To identify candidate neurons for CEES-mediated respiratory effects, we studied colocalization of PRV-152 (putative respiratory interneurons) and c-Fos (an immediate early gene likely activated by CEES) and colocalization of somatostatin (also a possible marker of respiratory interneurons in the cervical spine). To conduct these studies, animals were perfused transcardially with PBS followed by 4% paraformaldehyde (pH 7.3) at the end of each experiment. Tissue was extracted and post-fixed for 24 hours in 4% paraformaldehyde, placed in 30% sucrose for cryopreservation, and placed into 10% gelatin and frozen. Tissue was sectioned into 30 μm coronal slices using a cryostat (Leica CM 1800). Standard immunofluorescence techniques were performed. PRV-152 encodes a GFP tag for localization. This signal was amplified using an antibody against the GFP protein. Tissue was incubated in primary antibodies for 48 hours (anti-c-Fos (1:1000), Abcam (Cambridge, MA) ab190289; anti-green fluorescent protein (GFP; (1:2500) Abcam, ab13970, mouse anti-somatostatin (1:50), Genetex (Irvine, CA), GTX71935). Tissue was subsequently incubated in secondary antibodies against the host of the primary antibody for 1 hour at room temperature (Cy3, Cy2, and Cy5 Jackson ImmunoResearch, West Grove, PA). Negative controls, in which tissue underwent the same protocol, but did not include a primary antibody, were used to confirm optimal antibody dilution and imaging settings. Image J was used to quantify cell expression and co-localization. Images were down sampled into 8-bit resolution to facilitate cell counting, and the Threshold and Analyze Particle tools were used to quantify cells expressing c-Fos, GFP, and DAPI expression. GFP and c-Fos images were acquired and quantified with 10 x magnification. Co-localization was quantified by merging the two expression images from ImageJ. Co-localization was considered positive when expression distributions within a cell were overlapping. The dorsal motor nucleus, which innervates organs relating to the gastrointestinal tract located in the abdominal cavity, was explored in each animal to verify that PRV-152 did not leak into the abdominal space where it might have led to non-specific spinal labeling.

C3-C6 cervical epidural electrical stimulation induced respiratory activity

Seven animals underwent CEES at multiple cervical levels to map the respiratory responses to EES delivered along the cervical spinal cord (C3, C4, C5, and C6). Three animals underwent CEES at a constant

location (C2/3) to determine the respiratory response at different stimulation amplitudes between 0.5-3 mA. (data not shown). Each animal was anesthetized and prepared as described above, but did not receive PRV-152 injections into the diaphragm prior to the CEES studies.

Inhibitory DREADD expression in somatostatin-expressing neurons

Two viral constructs were injected to achieve selective expression of the inhibitory DREADD, HM4D(Gi) in somatostatin (SST)-expressing neurons. Dual AAV intraspinal injections were performed in 27 animals (n = 27). Rats that received both viral constructs, SST-Cre and HM4D(Gi), were divided into a CNO - test group (AAV-SST-Cre+AAV-hM4D(Gi)+CNO, n = 9 of 27) and a vehicle control group that received DMSO (AAV-SST-Cre+AAV-HM4D(Gi)+DMSO, n = 9 of 27). Additionally, nine animals were injected with an AAV lacking the Cre construct (AAV-SST-eGFP) and the AAV- hM4D(Gi)-mCherry to serve as a viral expression control without expressing the inhibitory hM4D(Gi) or mCherry. These animals received CNO and CEES as described below.

Each animal was anesthetized with isoflurane and placed prone on a water-circulating heating pad to prevent hypothermia. Surgery was performed aseptically: the skin was shaved and prepped with 70% alcohol and Betadine. A vertical incision was made from the base of the skull to the top of the shoulder blades to gain access to the dorsal spine. The acromiotrapezius and paraspinal muscles were separated to expose the spinal column. A laminectomy of the cervical level 3 (C3) was performed. Four intraspinal microinjections of the AAV serotype 2 (AAV2) carrying Cre under control of the SST promoter and expressing enhanced green fluorescent protein (eGFP): AAV2-SST-eGFP-T2A-iCre-WPRE (Vector Biolabs, Malvern PA; $3.0x10^{12}$ gc/mL) were made. An additional AAV carrying a double-floxed inhibitory DREADD receptor protein, hM4D(Gi), fused to the mCherry protein (mCherry) [94]: AAV-hSyn-DIO-hM4D(Gi)-mCherry (Addgene; $2.5x10^{12}$ gc/mL) was mixed with the other AAV virus and the injections were performed (n = 18 of 27). To control for any effect that expression of the viral vector may have had, 9 of the 27 animals received intraspinal injections of a control adenoviral vector that did not include the Cre cassette, AAV2-SST-eGFP-WPRE (Vector Biolabs, $3.0x10^{12}$ gc/mL) and the same double floxed

AAV-hSyn-DIO-hM4D(Gi)-mCherry (Addgene; $2.5x10^{12}$ gc/mL). Injections were targeted rostrally to C2/3 and caudally to C3/4. Injections were made bilaterally ~ 1 mm medial/lateral from the posterior central vein. All injections were performed at a rate of 2 nL/sec at a depth of 0.5-1.0 mm from the dorsal surface using a micropressure injector (WPI, Sarasota FL, Micro2T) [95]. A 5-minute period elapsed before the needle was withdrawn from the tissue to minimize leakage. Each animal received buprenorphine (0.05 mg/kg) prior to closing the surgical incision. The muscle was closed with 5-0 Vicryl, and 5-0 Ethilon was used to close the skin tissue. Carprofen (5 mg/kg) was administered, as needed, for dermatitis when it developed around the incision site.

Effect of epidural electrical stimulation during inhibition of somatostatin-expressing neurons

Three weeks elapsed between the time of AAV-hM4D(Gi) plus AAV-SST-Cre-eGFP injections, and the study of respiratory activity during CEES with or without activation of the inhibitory DREAAD channel. For each CEES study, the animal was anesthetized with urethane (1200 mg/kg) and alpha-chloralose (30 mg/kg) and prepared with diaphragm EMG electrodes, a tracheostomy, and a laminectomy, as described above. Animals underwent sham and active CEES at C3 to define the stimulation amplitude to use and the typical respiratory response of each animal prior to drug or vehicle injection. Amplitudes were selected so respiratory responses were optimized without overt upper extremity activity, ranging from 1.5-2.0 mA. After successful respiratory modulation by CEES, each animal was given 1 mg/kg CNO (in 1.5% DMSO) intraperitoneally to activate the hM4D(Gi) or a control injection of 1.5% DMSO to assess the effects of the vehicle. Animals underwent sham trials of CEES prior to and 20- and 60-minutes post-drug delivery. Active stimulation trials were conducted every 20 minutes for 100 minutes post-drug delivery. Animals that had minimal EES respiratory modulation prior to drug delivery were excluded from the data analysis (n = 3 of 27).

Quantification of hM4Dgi-mCherry expression

At the end of the experiment, the animals underwent transcardial perfusion and tissue preparation for immunohistochemical studies as described above. Thirty μm coronal slices from the cervical spine were

incubated in primary antibodies for 24 hours at 4°C, anti-mCherry (1:200) GeneTex (Irvine, CA), GTX128508; rabbit anti-SST (1:50) Bioss (Boston, MA), 8877R). Incubation in secondary antibodies (1:200) was performed for 1 hour at room temperature. Images with 16-bit resolution were acquired using an Echo Revolve (Echo, San Diego, CA 92126). Image J was used to quantify cell expression and co-localization as described above. DAPI and mCherry images were acquired and quantified at 20 x magnification.

Data Analysis

In the first study using PVR-152 and c-Fos activation, respiratory and EMG data were obtained with DataView (Dr. W. J. Heitler, University of St. Andrews). End-tidal CO_2 ($PETCO_2$) values were obtained using a Kent Scientific (Torrington, CT) capnograph and recorded using LabChart (ADInstruments, New Zealand). Data visualization, post-processing, and extraction were performed with Matlab (MathWorks). Tidal volumes were calculated from the integral of the inspiratory flow. Diaphragm activity during C2/3 CEES was calculated as the average integral of diaphragm EMG activity and expressed as a percent of the difference from baseline activity. Statistics were performed in R Studio (Boston, MA). C2/3 EES respiratory frequency, minute volume, and $PETCO_2$ were analyzed using a two-way repeated measures ANOVA in which treatment condition versus sham and time (serial measurements) were within-subjects factors. Tukey's Honestly Significant test was performed for post-hoc analysis. To analyze c-Fos and PRV-152 expression, we used a two-way ANOVA with Sham/Stim as a between-subject factor and cervical level (C1-C7) as a within-subject factor.

In the study of mapping the responses to CEES, the respiratory frequency, minute volume, and $PETCO_2$ during CEES at C3 – C6 were analyzed with discrete two-way ANOVAs for each location tested (C3-C6). Treatment and time were within-subject factors. To explore if any one location initiated an increase in respiratory activity more than another, a 3-way ANOVA was explored. We found no significant interaction between time, location, and condition among the 4 cervical levels tested. Yet, individual 2-way ANOVA results suggest differences in the modulation of respiratory activity by CEES along the rostral to caudal

axis of the cervical spinal cord. That is, more rostral levels tended to increase frequency while at caudal levels, a significant frequency increase was not observed but a minute volume increase was.

To analyze the results of DREADD activation during CEES, we analyzed respiratory activity as a percent change calculated as the frequency or minute volume change during the 30s of Sham/Stim (Intra) compared to the frequency or minute volume of the 30 s immediately prior (Pre) divided by the 30 s immediately prior (Pre) multiplied by 100. The percent change data were analyzed with a mixed effects model with treatment group (CNO or vehicle) as a between-subjects factor and time as a within-subjects factor. Multiple comparisons were made to compare each group to its own Sham condition and tested with Dunnett's test when the mixed effects model indicated that paired tests were warranted.

Results

Dorsal epidural electrical stimulation at C2/3 increases ventilation

To investigate respiratory responses to cervical spinal stimulation in anesthetized rats, CEES was applied to the dorsal epidural surface of the spinal cord at C2/3 using a continuous 30 Hz monophasic waveform for 30 s with amplitudes ranging from 1.5 to 2.5 mA (Figure 1). There was a significant interaction between condition and time for the respiratory frequency ($F_{(2, 20)}$ = 12.15, df = 2, p = 0.0004). CEES at C2/3 significantly increased the respiratory rate during stimulation compared to the baseline period (p = 0.0001, data shown in Table 1), as shown in Figure 1B. Sham trials, in which the electrodes were placed on the epidural surface, but no current was delivered, had no effect on the respiratory rate compared to baseline (p>0.05, Table 1, Figure 1B). There was a significant interaction between condition and time for minute volume ($F_{(2, 16)}$ = 21.73, df = 2, p = 0.0001). Minute volume was significantly increased during CEES trials at C2/3 compared to baseline (p = 0.0001 Table 1, Figure 1C). There was no effect on minute volume during sham trials compared to baseline (p>0.05).

Diaphragm muscle activity and PET_{CO2} values were monitored to assess the ventilatory effect of EES, as shown in Figure 1D-E. A significant interaction between condition and time was observed for $PETCO_2$ ($F_{(2,}$

$_{36)}$ = 23.7, df = 2, p < 0.0001). $PETCO_2$ was significantly decreased during CEES compared to baseline (p = 0.002, as shown in Figure 1D). Sham trials had no effect on $PETCO_2$ values. Due to stimulation artifact, diaphragm activity could only be identified in six animals during stimulation. Nonetheless, there was a significant interaction between condition and time for the diaphragm activity, expressed as a percent of the difference between the activity that was calculated for the Intra and Pre periods ($F_{(1, 10)}$ = 9.24, df = 1, p = 0.01). CEES significantly increased diaphragm activity compared to sham trials (Figure 1E).

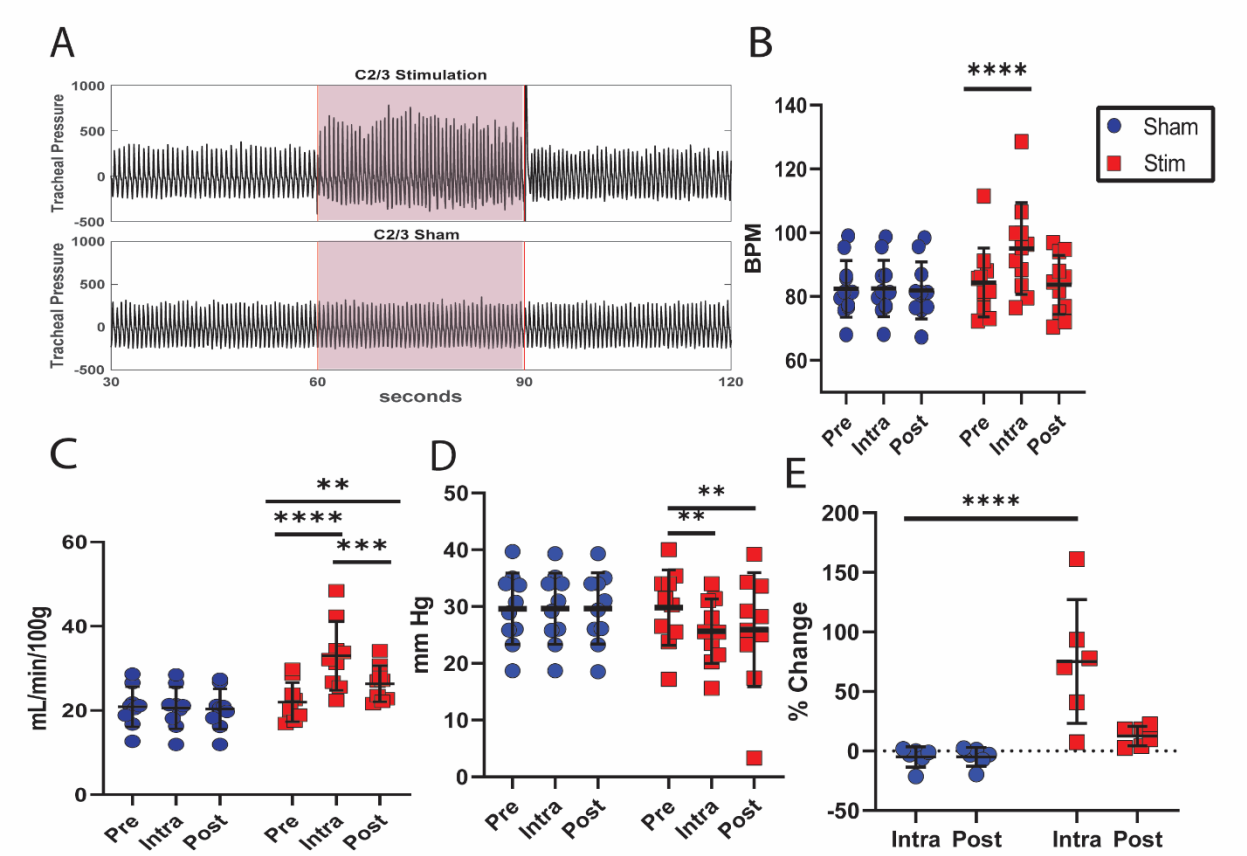

Figure 2.1: Cervical epidural stimulation at the intersection of C2 and C3 increases respiratory activity in anesthetized rats. A) Example of tracheal pressure recording from one animal receiving both Stimulation and Sham stimulation. B) C2/3 CEES increases respiratory frequency compared to baseline (Pre). Sham stimulation had no effect on respiratory frequency (n = 11). C) C2/3 CEES increased respiratory minute volume compared to baseline. Sham stimulation had no effect on minute volume (n=10) D) PETCO2 was signifcantly decreased during and for 30 s after CEES (Post) compared to baseline (n=10). E) Diaphragm muscle activity as a percentage of the activity from baseline was increased during stimulation compared to Sham conditions (n=6). Data was analyzed with a two-way ANOVA and Tukey's Honestly Signifcant test was used to correct for multiple comparisons. ** p<0.01 ***p<0.001 ****p<0.0001

Table 2.1 CEES at C2/3 Data			
variable	Baseline (pre-) Mean ± SD	During stimulation (intra-) Mean ± SD	After stimulation (post-) Mean ± SD
Condition: CEES			
Respiratory frequency (breaths/min)	84.4 ± 10.8	95.1 ± 14.4****	83.7± 9.3 n.s.
Minute ventilation (mL/min/100 g)	21.99 ± 4.66	32.99 ± 8.21****	26.34 ± 4.26 **
Integrated diaphragmatic EMG (percent change	0 ± 0	75.2 ± 52.0*	12.5 ± 8.27 n.s.
PETCO2 (mm Hg)	29.80 ± 6.65	25.63 ± 5.67**	25.93 ± 10.07**
Condition: Sham			
Respiratory frequency(breaths/min)	82.4 ± 8.9	82.5 ± 8.9	81.9 ± 8.9
Minute ventilation (mL/min/100 g)	20.99 ± 4.76	20.61 ± 4.76	20.33 ± 4.80
Integrated diaphragmatic EMG (percent change)	0 ± 0	-4.9 ± 8.4	-4.9 ± 7.9
PETCO2 (mm Hg)	29.64 ± 6.27	29.56 ± 6.29	29.66 ± 6.26

While stimulation modulated respiratory behavior during stimulation, the frequency and diaphragm increases did not last after stimulation ended, and all variables returned to near baseline levels (Figure 1B and E, $p>0.05$). Minute volume remained significantly elevated compared to baseline levels (Figure 1C, $p = 0.006$), and PET_{CO2} values, remained significantly decreased post-stimulation (Figure 1D, $p = 0.001$), reflecting the slower dynamics of CO_2 gas exchange. These results indicate that, similar to mice, dorsal CEES increases respiratory activity in rats, and some, but not all, respiratory effects persist after stimulation ended, though all variables tended to decay back to baseline over ~ 90 s [92].

Epidural electrical stimulation activated cervical spinal sensory and respiratory interneurons

Since CEES modulated respiratory behavior in anesthetized rats, we explored the location and identification of the neurons being activated by CEES at C2/3. To investigate spinal neurons connected to the phrenic motor neurons through polysynaptic circuits that may be activated by EES, the retrograde tracer, pseudorabies virus (PRV-152), was injected bilaterally into the diaphragm muscle. The incubation time used for this experiment (64-66 hours) was sufficient to label putative spinal interneurons including those

observed before and after brainstem pre-motor neuron labeling [67, 93]. For studies of c-Fos activation, a control group of animals received PRV-152 injections into the diaphragm and 64-66 hours later a laminectomy. These animals were maintained for at least an hour after conclusion of the laminectomy to serve as a Sham treatment group. Another group of animals, received a laminectomy followed by six CEES (Stim) and sham (Sham) trials at C2/3, each separated by a period of 8-10 minutes to allow respiratory activity to return to baseline (data included in Figure 1). The animals in the Stim group, survived for at least one hour past the mid-way point of stimulation. For each group, tissue was stained with antibodies against the immediate early transcription factor protein, c-Fos, and anti-GFP to visualize PRV-152 (Figure 3). There was minimal to no GFP signal observed in the dorsal motor nucleus, as shown in Supplementary Figure 1A, indicating that the staining of neurons in the spine originated from the diaphragmatic innervation. GFP signal was observed in the ventrolateral medulla demonstrating that PRV-152, through retrograde transfection, entered phrenic motor neurons and moved 'upstream' to infect putative spinal interneurons and other rostral elements of the respiratory control system [93], Supplementary Figure1B. Most c-Fos positive neurons were localized to the dorsal horn at each cervical spinal level examined, specifically in laminae 1-3 and to a lesser extent laminae 4-6. c-Fos and PRV-GFP-labeled cells were counted, and the extent of co-localization in laminae 2-5 assessed, as shown in Figure 2. There was a significant interaction between stain (c-Fos or GFP) and condition (Stim or Sham) within levels C3-5 (phrenic nucleus- $F_{(2, 64)} = 16.73$, df = 2, p = 0.0001) and C6-T1 ($F_{(2, 32)} = 4.91$, df = 2, p = 0.01). There was significantly more c-Fos expression in tissue within the C3-5 (49.1 ± 40.74 cells, p = 0.018) and C6-7 regions (14.13 ± 8.32 cells, p = 0.007), compared to sham animals in a comparable region (C3-5 3.08 ± 3.05, C6-7 0.4 ± 0.70), as shown in Figure 2E. c-Fos activation was higher at levels closer to the site of the CEES application (C2/3). At all levels, there were more neurons with co-localized c-Fos and GFP expression in the active CEES condition, but this was not significantly different from sham condition in which each animal breathed normally under anesthesia without CEES (p>0.05). There were no differences in GFP expression between conditions at C1-2 (Sham 27.38 cells; SD ± 14.39 cells, Stim 40.75 cells; SD ±

26.20 cells), C3-5 (Sham 31.13 cells; SD ± 19.33 cells, Stim 38.70 cells; SD ± 25.67 cells), and C6-7 (Sham 40.30 cells; SD ± 18.50 cells, Stim 30.75 cells; SD ± 23.89 cells). These results suggest that CEES activates an expansive network of respiratory and non-respiratory cells within the spinal cord, including neurons active in the baseline respiratory state.

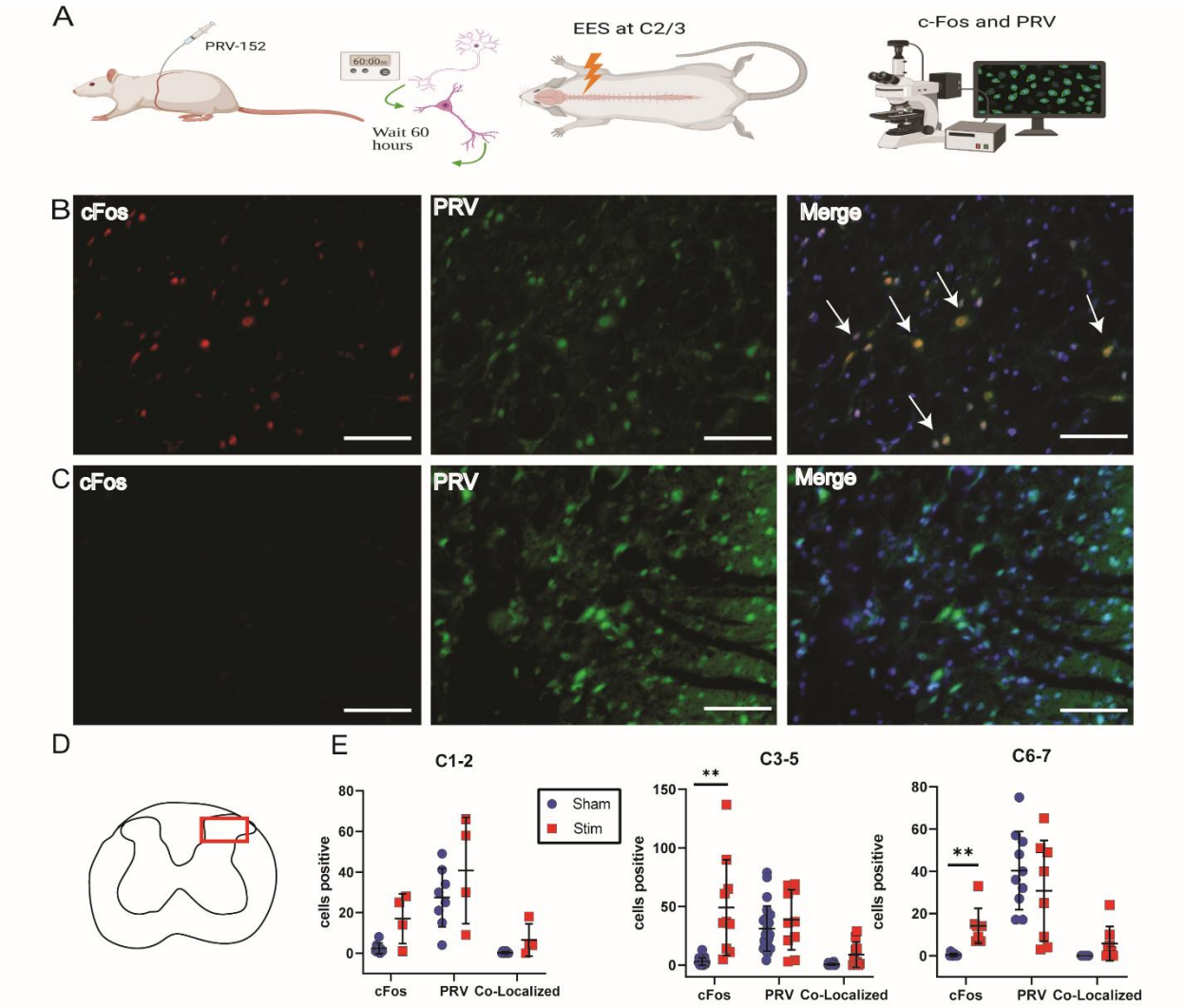

Figure 2.2: c-Fos expression in respiratory interneurons expressed in animals that received 30Hz CEES at C2/3. A) Experimental design. B) c-Fos expression observed co-localized with PRV expression in the dorsal cervical spinal cord of stimulated animal at C2/3. C) Little to no c-Fos expression in animals that received sham surgery. D) PRV-152 was given 60 hours prior to stimulation resulting in at least 2 synaptic jumps. E) c-Fos expression in laminae 3-5 was significantly increased within cervical levels C3-5 (phrenic nucleus) compared to animals only recieving PRV-152 retrograde tracing and sham surgery. No differences were observed between groups for expression of PRV-152. There was not a significant difference between groups in the co-localization of c-Fos and PRV-152 expression. All images were acquired at 20x magnification. Scale bar = 70 um. A and D created with BioRender.com

Somatostatin-expressing neurons activated by C2/3 epidural electrical stimulation

Somatostatin (SST) is expressed in neurons within brainstem respiratory nuclei that influence the respiratory phase and timing of firing among neuronal subtypes within the respiratory pattern generator [27, 29, 96]. Given this and its known expression in sensory neurons within the spinal cord, we explored SST expression in the dorsal regions of the spine that also highly expressed c-Fos after CEES. We found that SST expression was extensive in regions where CEES-induced and respiratory-related c-Fos expression co-localized with putative respiratory interneurons (PRV-125-positive cells; i.e., laminae 1-3, as shown in Figure 3.

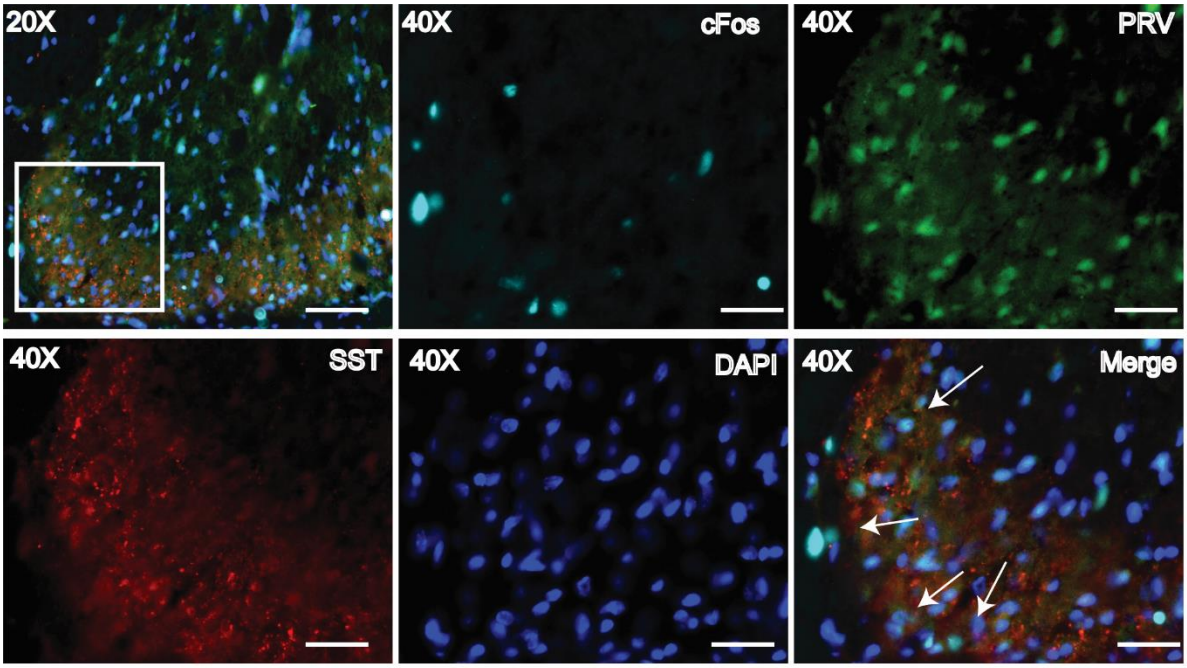

Figure 2.3: c-Fos positive putative respiratory interneurons were observed with and around SST expression in the dorsal horn of the cervical spinal cord. Arrows point to cFos-PRV positive neurons near SST expression. 20x scale bar equals 70 um. 40x scale bar equals 30 um.

Epidural electrical stimulation applied along the cervical spinal cord increases ventilation

To gain insight into the differences in sites of CEES and respiratory modulation along the cervical spinal cord, where phrenic motor neurons reside, CEES at levels 3-6 (C3-C6) was evaluated (data shown in Table 2, Figure 4). There was a significant interaction between time and condition for respiratory frequency at C3 ($F_{(2, 16)}$ = 4.59, df = 2, p = 0.02) and C4 ($F_{(2\ 28)}$ = 4.15, df = 2, p = 0.02). Respiratory rate was significantly

greater during CEES when applied at C3 ($p = 0.01$) and C4 ($p = 0.03$) compared to baseline (Figure 4A). In addition to frequency modulation, there was a significant interaction between condition and time for minute ventilation when CEES was applied at C4 ($F_{(2, 14)} = 5.01$, df = 2, $p = 0.01$). Minute ventilation was significantly greater during CEES at C4 compared to baseline ($p = 0.001$, Figure 4B). CEES applied to C5 and C6 tended to increased frequency but it was not significantly different from sham values. However, there was a significant interaction of condition and time for minute volume when CEES was applied at C5 ($F_{(2, 10)} = 6.34$, df = 2, $p = 0.02$) and C6 ($F_{(2, 10)} = 4.19$, df = 2, $p = 0.047$) When CEES was applied to C5 and C6 there was an increase in minute ventilation compared to baseline (C5 $p = 0.003$, C6 $p = 0.005$, Figure 4B). There was a significant interaction of condition and time for $PETCO_2$ when CEES was applied at C3, C5, and C6. $PETCO_2$ decreased during stimulation at C3 ($p = 0.0004$), C5 ($p = 0.007$), and C6 ($p = 0.05$) when compared to baseline values, as shown in Figure 4C. $PETCO_2$ values during CEES at C4 were lower but not significantly different from baseline ($p = 0.087$). For all levels, sham stimulation had no effect on frequency, minute volume, and $PETCO_2$ (data shown in Table 2). In conclusion, CEES increases ventilation in rats and the modulation along the cervical spinal cord varies, similar to what was observed in mice [92]. Differences in respiratory modulation by CEES along the cervical spinal cord could be exploited for therapeutics to enhance respiratory drive.

Table 2.2 CEES C3-C6

Variable	Location	Baseline (pre-) Mean ± SD	During stimulation (intra-) Mean ± SD	Post stimulation (post-) Mean ± SD
Condition: CEES				
Respiratory frequency (breaths/min)	C3	84.2 ± 10.0	96.5 ± 6.1*	91.9 ± 9.3
	C4	84.4 ± 10.4	94.8 ± 13.9*	88.6 ± 8.3
	C5	85.8 ± 10.6	102.1 ± 10.4 n.s.	95.7 ± 7.3
	C6	85.2 ± 10.7	93.0 ± 9.8 n.s.	87.3 ± 8.1
Minute ventilation (mL/min/100 g)	C3	19.09 ± 5.01	28.36 ± 16.56n.s.	20.75 ± 7.34
	C4	16.50 ± 9.36	28.22 ± 15.83****	21.54 ± 12.23

	C5	20.94 ± 8.75	32.08 ± 7.77**	26.16 ± 10.70
	C6	15.86 ± 8.65	26.61 ± 18.68*	20.02 ± 12.97
$PETCO_2$ (mm Hg)	C3	29.19 ± 2.01	25.64 ± 3.66***	27.71 ± 3.31
	C4	29.37 ± 4.34	26.24 ± 4.30 n.s.	27.89 ± 4.24
	C5	29.86 ± 3.38	25.29 ± 4.64**	28.90 ± 3.96*
	C6	29.59 ± 2.96	26.83 ± 3.48*	28.48 ± 3.16*
Condition: Sham				
Respiratory frequency (breaths/min)	C3	81.1 ± 6.7	81.2 ± 6.5	80.9 ± 6.2
	C4	85.2 ± 10.2	85.2 ± 10.1	85.6 ± 11.2
	C5	85.8 ± 4.5	86.3 ± 5.2	86.2 ± 5.0
	C6	84.9 ± 7.7	81.9 ± 6.9	84.7 ± 8.4
Minute ventilation (mL/min/100 g)	C3	16.33 ± 6.40	16.34 ± 7.16	16.49 ± 6.71
	C4	19.57 ± 7.43	18.64 ± 6.59	18.15 ± 7.11
	C5	19.88 ± 9.88	19.93 ± 10.15	18.79 ± 11.54
	C6	15.38 ± 6.96	15.69 ± 7.67	15.86 ± 7.62
$PETCO_2$ (mm Hg)	C3	29.66 ± 2.03	29.76 ± 2.20	29.63 ± 2.16
	C4	30.46 ± 2.84	30.66 ± 2.83	30.81 ± 2.83
	C5	31.44 ± 3.10	31.31 ± 2.92	31.41 ± 2.94
	C6	30.12 ± 3.21	30.06 ± 3.32	29.91 ± 3.35

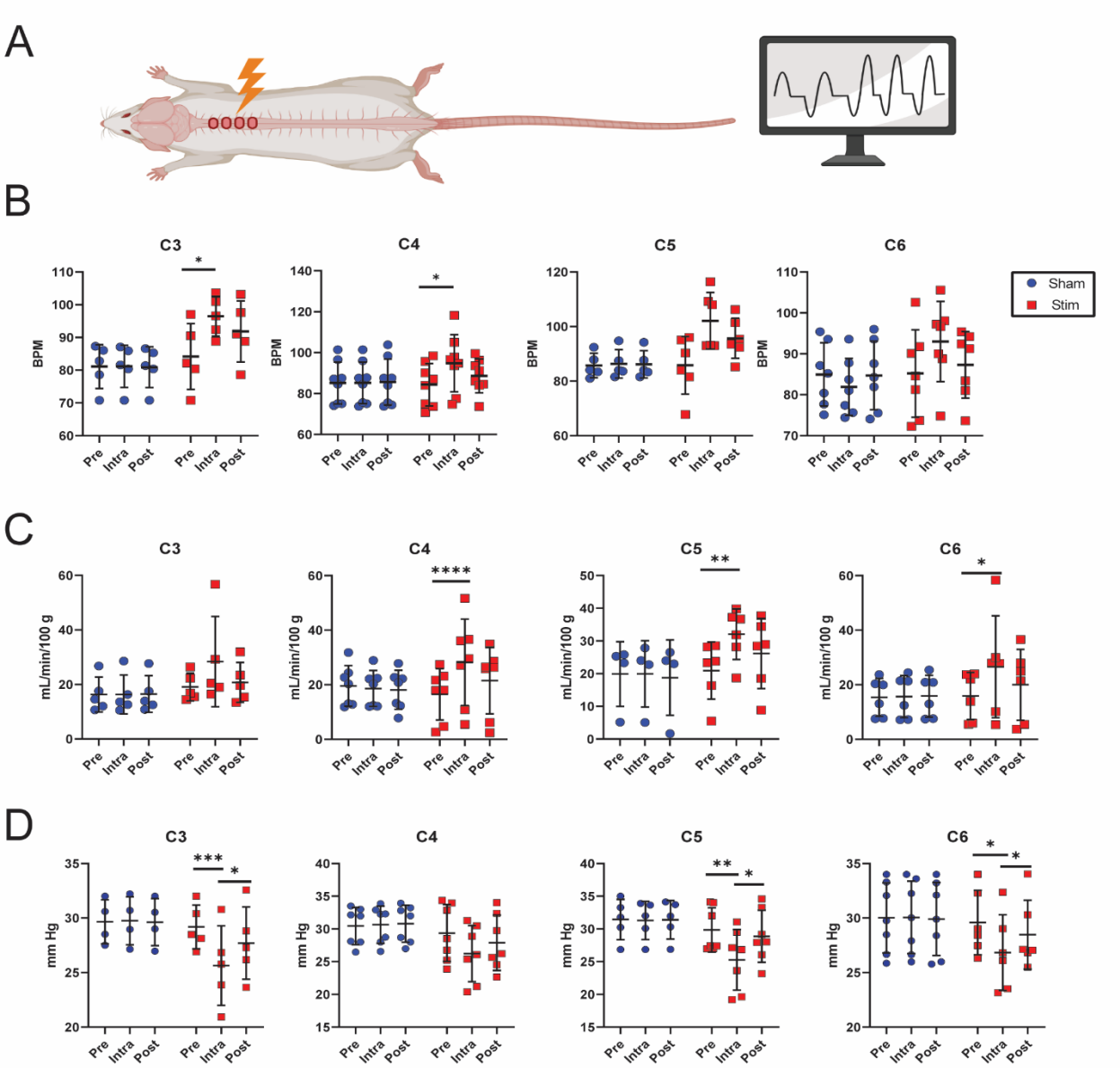

Figure 2.4: Cervical epidural stimulation at cervical levels 3-6. A) Animals were anesthetized and CEES applied while respiratory activity monitored. B) CEES applied at C3 and C4 increases respiratory frequency compared to baseline frequency. C) CEES applied at C4, C5, C6 increases minute volume (MV) compared to baseline MV. D) PETCO2 was significantly decreased during EES when applied at C3, C5, and C6. Data was analyzed with a 2-way ANOVA with time (Pre, Intra, Post) and condition (Stim/Sham) for each location. Bonferroni test was applied to account for multiple comparisons. C3 n = 5, C4 n = 7, C5 n = 6, C6 n = 6. * p< 0.05, ** p<0.01, ***P<0.001 Created with BioRender.com

Silencing SST-expressing neurons decreases the effect of cervical epidural electrical stimulation

Since SST expression co-localized with CEES-induced c-Fos expression, and SST-positive neurons participate in respiratory neurogenesis in the brainstem, we explored the role of SST-expressing neurons in

the cervical spine in CEES-induced respiratory activation. We selectively expressed the chemogenetic inhibitory Designer Receptor Exclusively Activated by Designer Drugs (DREADD), hM4D(Gi), in SST cells in the cervical spinal cord. Selective expression of hM4D(Gi) in SST cells was probed and verified by colocalization of mCherry expression and SST expression in the dorsal horn of the cervical spine; see Supplementary Figure 2. CNO was used to silence SST-expressing cells that also expressed hM4D(Gi). We studied the following groups of animals: AAV-SST-Cre+AAV-hM4D(Gi)+CNO, AAV-SST-Cre+AAV-hM4D(Gi)+DMSO, AAV-SST-eGFP+AAV-hM4D(Gi)+CNO. There was a significant interaction between group and time for respiratory frequency ($F_{(12, 123)} = 2.78$, $p = 0.002$). All groups responded with a significant increase in respiratory frequency during CEES at C3 prior to drug delivery compared to sham trials (AAV-SST-Cre+AAV-hM4D(Gi)+CNO $p = 0.001$, AAV-SST-Cre+AAV-hM4D(Gi)+DMSO $p = 0.005$, AAV-SST-eGFP+AAV-hM4D(Gi)+CNO $p = 0.01$, Figure 5). Rats that were in either control group (AAV-SST-Cre+AAV-hM4D(Gi)+DMSO or AAV-SST-GFP + AAV-hM4D(Gi) + CNO) continued to show significant frequency increases at all time points tested (20-100 min post-DMSO/CNO delivery). When CEES was applied in the active experimental group (AAV-SST-Cre+AAV-hM4D(Gi)+CNO), the increase in respiratory frequency was diminished or ablated at 40, 60, and 80 minutes post-CNO delivery, as see in Figure 5A and B). This reduction was sufficient to return the frequency to values equal to those observed in the sham group (40- $p = 0.16$, 60- $p = 0.41$, 80- $p = 0.18$). Volumes of AAV vectors ranged from 100-700 nL per injection, and these volumes were compared to maximum responses observed during the respiratory CEES experiments. Volumes of 400 nL and above caused maximal inhibition, resulting in close to zero change from baseline during stimulation. There was no significant interaction between time and group for minute volume responses among groups over time, similar to what was seen in stimulation at C3 in the prior experiment (Figure 5D). However, we did find a significant interaction between group and time for changes in $PETCO_2$ ($F_{(12, 108)} = 1.92$, $df = 12$, $p = 0.039$). Prior to CNO/DMSO treatment all groups showed a significant decrease in $PETCO_2$ (AAV-SST-Cre+AAV-hM4D(Gi)+CNO $p = 0.004$, AAV-SST-Cre+AAV-hM4D(Gi)+DMSO $p = 0.0003$, AAV-SST-eGFP+AAV-hM4D(Gi)+CNO $p =$

0.004, Figure 5E). After CNO treatment, the reduction in $PETCO_2$ values were not significantly different from sham in the active experimental group. The two control groups continued to show a significant decrease in $PETCO_2$ when CEES was applied throughout the 100 minutes of the experiment. These results suggest that, close to the site of stimulation at C3, respiratory frequency modulation resulting in functional gas exchange by CEES is dependent upon neurons expressing SST in the cervical spinal cord.

Expression of mCherry was quantified across cervical levels to determine where hM4D(Gi) was expressed. The majority of mCherry was expressed within the dorsal horn, as shown in Figure 6. Rostral brainstem slices were examined for mCherry expression to determine the extent of the brainstem contribution to hM4D(Gi)-mediated inhibition during CEES modulation of respiration. There was scant mCherry expression observed within the brainstem, as shown in Supplementary Figure 3. This suggests that the majority of hM4D(Gi) was expressed in the cervical spinal cord, diminishing the likelihood that inhibition of brainstem respiratory neurons contributed to the respiratory inhibition when hM4D(Gi) was activated by CNO. Thus, the hM4D(Gi) acted by inhibiting the activity of SST-expressing dorsal spinal neurons (likely interneurons) to occlude the excitatory effect of CEES on respiration.

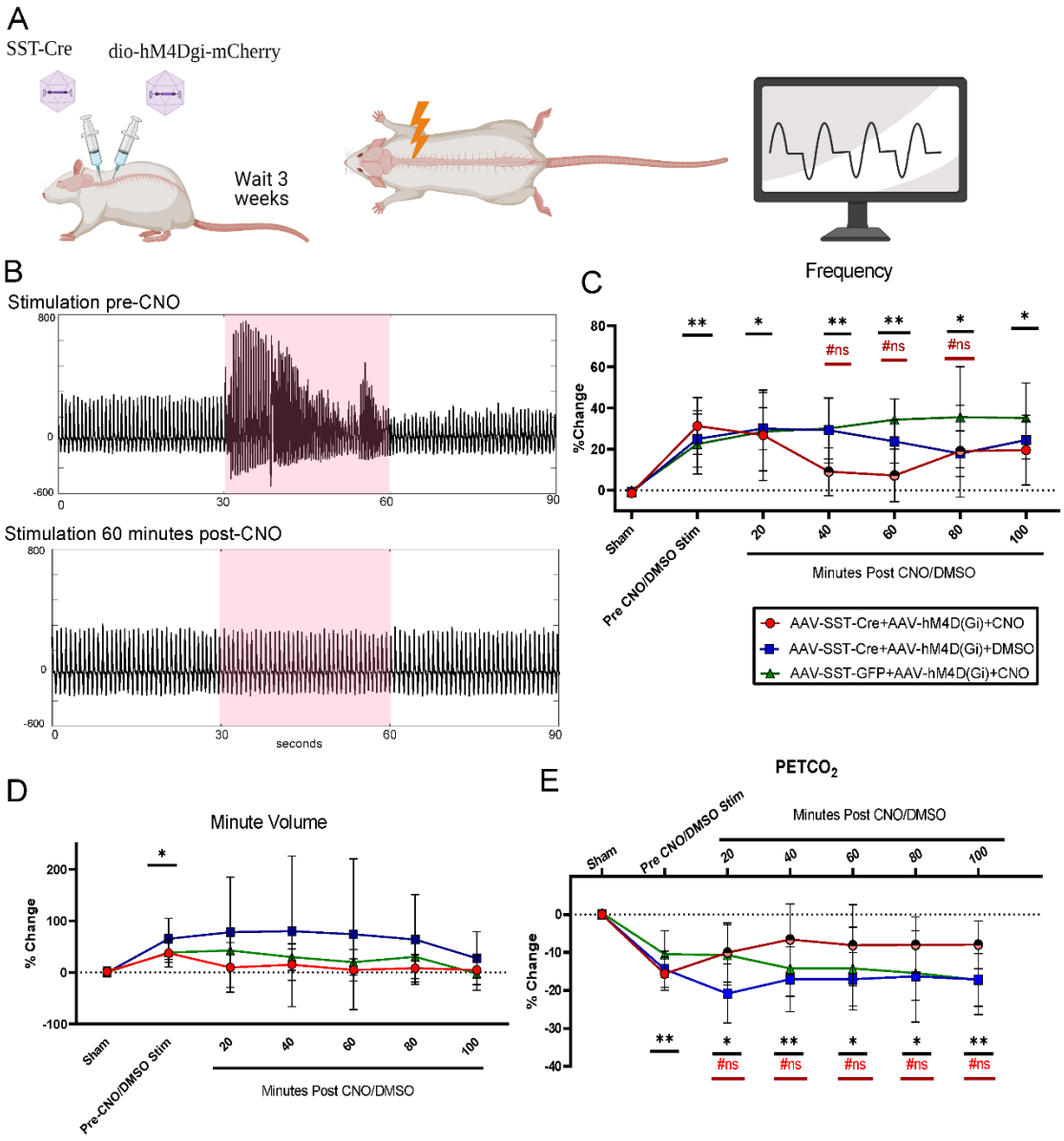

Figure 2.5: hM4D(Gi) was expressed in SST neurons within the cervical spinal cord and CEES at C3 was conducted prior to and after CNO/DMSO (1 mg/kg in 1.5% DMSO) IP injection. A) Experimental Design. Wild-type rats were injected with dual AAV viral injections to express hM4D(Gi) in SST-expressing neurons. B) Example of raw tracheal pressure from an animal that received 30 s of CEES, red rectangle, prior to CNO and 60 minutes post-CNO. C) Mean and standard deviation of respiratory frequency modulation analyzed as a percent change from the baseline respiratory frequency. D) Minute volume modulation. E) Mean of PETCO2 change during CEES across time. Data was analyzed with mixed effects model with group as a between subjects factor and time as a within subjects factor. Dunnett's test was used for multiple comparisons. #ns specifies AAV-SST-Cre+AAV-hM4D(Gi)+ CNO comparison to Sham stimulation. n=8 per group. * p< 0.05, ** p< 0.01. Created with BioRender.com

Table 2.3				
Variable	Group	During EES- Frequency Percent change from baseline (% ± SD)	During EES- Minute Volume Percent change from baseline (% ± SD)	During EES- $PETCO_2$ Percent change from baseline (% ± SD)
Sham	AAV-SST-Cre+AAV-hM4D(Gi)+CNO	-1.34 ± 2.07	1.67 ± 8.77	0.02 ± 0.33
	AAV-SST-Cre+AAV-hM4D(Gi)+DMSO	-0.88 ± 1.80	-0.26 ± 4.13	0.02 ± 0.41
	AAV-SST-eGFP+AAV-hM4D(Gi)+CNO	-0.17 ± 1.20	0.28 ± 4.05	0.45 ± 0.78
Pre CNO/DMSO Stim	AAV-SST-Cre+AAV-hM4D(Gi)+CNO	31.29 ± 13.80	37.55 ± 26.59	-15.62 ± 4.33**
	AAV-SST-Cre+AAV-hM4D(Gi)+DMSO	24.96 ± 13.84	65.28 ± 39.67	-14.40 ± 4.81***
	AAV-SST-eGFP+AAV-hM4D(Gi)+CNO	22.53 ± 14.60	38.76 ± 19.41	-10.45 ± 6.18**
20 min Post CNO/DMSO	AAV-SST-Cre+AAV-hM4D(Gi)+CNO	26.82 ± 22.09	9.82 ± 48.03	-10.01 ± 7.86 n.s.
	AAV-SST-Cre+AAV-hM4D(Gi)+DMSO	30.03 ± 10.13	78.08 ± 106.78	-20.80 ± 7.75***
	AAV-SST-eGFP+AAV-hM4D(Gi)+CNO	28.52 ± 19.05	42.51 ± 30.63	-10.66 ± 7.87*
40 min Post CNO/DMSO	AAV-SST-Cre+AAV-hM4D(Gi)+CNO	9.10 ± 11.63	15.05 ± 30.32	-6.56 ± 9.33 n.s.
	AAV-SST-Cre+AAV-hM4D(Gi)+DMSO	29.21 ± 15.86	80.05 ± 145.85	-17.03 ± 8.54**
	AAV-SST-eGFP+AAV-hM4D(Gi)+CNO	30.09 ± 14.76	29.80 ± 25.53	-14.20 ± 7.39**

60 min Post CNO/DMSO	AAV-SST-Cre+AAV-hM4D(Gi)+CNO	7.24 ± 12.83	4.93 ± 21.67	-8.04 ± 10.63 n.s.
	AAV-SST-Cre+AAV-hM4D(Gi)+DMSO	23.79 ± 10.48	74.29 ± 146.55	-17.03 ± 7.00**
	AAV-SST-eGFP+AAV-hM4D(Gi)+CNO	34.38 ± 10.07	19.98 ± 24.95	-14.18 ± 10.91*
80 min Post CNO/DMSO	AAV-SST-Cre+AAV-hM4D(Gi)+CNO	19.09 ± 22.39	8.27 ± 26.59	-7.96 ± 7.45 n.s.
	AAV-SST-Cre+AAV-hM4D(Gi)+DMSO	17.85 ± 11.12	63.89 ± 87.47	-16.29 ± 12.07*
	AAV-SST-eGFP+AAV-hM4D(Gi)+CNO	35.53 ± 24.60	30.36 ± 41.97	-15.42 ± 7.12**
100 min Post CNO/DMSO	AAV-SST-Cre+AAV-hM4D(Gi)+CNO	19.55 ± 17.01	5.01 ± 28.60	-7.89 ± 6.29 n.s.
	AAV-SST-Cre+AAV-hM4D(Gi)+DMSO	24.46 ± 9.13	27.62 ± 51.53	-17.10 ± 9.24**
	AAV-SST-eGFP+AAV-hM4D(Gi)+CNO	35.16 ± 17.06	-2.12 ± 32.58	-17.22 ± 6.97***

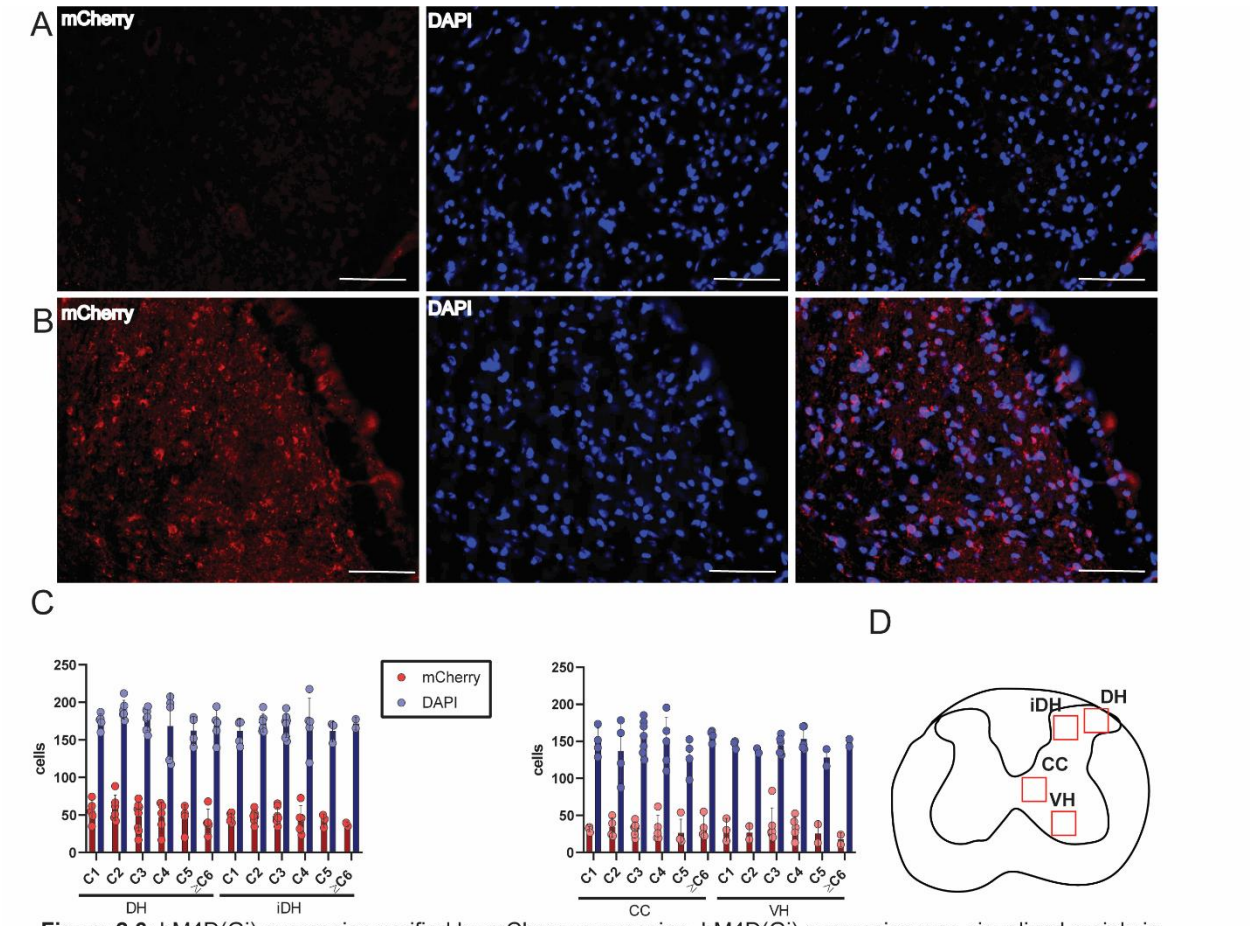

Figure 2.6: hM4D(Gi) expression verified by mCherry expression. hM4D(Gi) expression was visualized mainly in the dorsal horn. A) hM4DGi-mCherry expression in animals that received AAV-SST-GFP and AAV-dio-hM4DGi-mCherry. B) hM4DGi-mCherry expression in animals that received AAV-SST-Cre and AAV-dio-hM4DGi-mCherry. C) quantification of mCherry punctate. D) Diagram with red boxes around the areas used for analysis. All images were acquired at 20x magnification. Scale bar is 70 um.

Discussion

Respiratory activity increased during CEES of the dorsal spinal cord of anesthetized rats. Using c-Fos as a broad neuronal activation marker, we found CEES activated spinal neurons largely in the dorsal horn, suggesting involvement of a spinal sensorimotor circuit. To identify these activated neurons more specifically, PRV-152 was injected into the diaphragm and moved retrograde to trace putative respiratory spinal interneurons. We found c-Fos co-localized with PRV-152 labeled putative interneurons as well as non-PRV-152 labeled neurons. Additionally, there was no significant difference in co-localization of c-Fos and PRV-152 between sham and stimulated animals suggesting that a basal activation state existed in the

unstimulated condition, and CEES may have enhanced the already active spinal respiratory network plus non-respiratory spinal neurons, and likely both. c-Fos expression and PRV-152 co-localization was used to label cell-types involved in CEES-induced respiratory responses. Given that somatostatin (SST) is expressed in neurons in the brainstem expressing respiratory – related activity, we tested the hypothesis that SST-expressing neurons in the cervical spine might participate in the respiratory activation mediated by dorsal CEES [29, 97]. Co-localization of SST, c-Fos, and PRV-152 was observed in the dorsal horn, suggesting that SST-expressing neurons could be a candidate cell-type mediating respiratory responses elicited by CEES. Finally, using dual viral vector injections of Cre downstream of the SST promoter and hM4D(Gi) double-floxed vector, we selectively expressed the inhibitory DREADD, hM4D(Gi), in spinal SST-expressing neurons. After inhibition of the spinal SST-expressing neurons, CEES-induced increases in respiratory frequency and decreases in $PETCO_2$ were suppressed. Minute volume was suppressed as well following treatment with CNO, but minute volume tended to be more variable across all groups and no significant differences were seen. A decrease in minute volume modulation was observed across time for all groups, suggesting an attenuation to effects on minute volume over time. This will be an important aspect to consider and investigate for clinical use. Our results suggest that CEES activates a sensorimotor respiratory network that is dependent upon the activity of SST-expressing neurons in the cervical spinal cord to enhance respiratory activity.

Neuromodulation is a growing field that has shown promise both as a means to understand neural circuits better and as a therapeutic modality for disease states. Enhancing respiratory activity and minimizing diaphragm atrophy using different stimulation strategies for a variety of respiratory conditions with compromised respiratory activity is not new. Phrenic nerve stimulation, ventral or dorsal epidural stimulation along the cervical and thoracic spine, and intraspinal stimulation using bursts of stimulation (usually high frequency, > 100 Hz) to pace diaphragmatic muscle activity are approaches that have been explored by others [98-103]. In this experiment, we instead explored the effects of dorsal CEES on respiration, as this is an existing, low intensity, clinical approach for the treatment of pain that may be

repurposed to support respiratory activity. The stimulation frequency used in this set of experiments, continuous 30 Hz, was based on our previous work and the work of others showing that a mid-range frequency was beneficial in activating rhythmic spinal neural networks [92, 104, 105]. Based on previous studies, different stimulation frequencies (low vs high) can have variable effects that may be utilized for specific neurological conditions [106]. In this study, stimulation amplitudes were personalized for each animal at the beginning of the experiment and ranged from 1-2.5 mA. Given the constant 30 Hz frequency, these intensities were below direct activation of phrenic motor neurons as rhythmic contraction and relaxation of the diaphragm persisted. The researchers found that the amplitude needed to excite respiratory activity was dependent on several factors including anesthesia depth, animal size, and tissue resistance. In some animals, higher intensity stimulation inhibited respiratory activity and resulted in periods of apnea (D.C. Lu, unpublished data). This is likely due to direct motor neuron activation resulting in tetanic contraction since stimulation frequency was constant. Additionally, higher intensities resulted in tetanic contraction of the proximal upper limb muscles. We selected an amplitude that minimized extra-respiratory muscle contraction and maximized respiratory modulation. Therefore, the continuous, low-amplitude, low-frequency neuromodulation approach used in these experiments was below the threshold of motor activation and did not directly pace respiratory motor neurons. CEES, as administered in this study, likely provides a general increase in excitation to rostral respiratory central pattern generators and may increase the receptivity or tone of respiratory motor neurons to endogenous respiratory activity (resting membrane potential of phrenic and other respirator motor neurons).

Similar to nerves innervating peripheral muscles, the phrenic nerve has numerous types of afferents, Iα, Iβ, II, III (Iδ), and IV, and their activity can influence respiratory activity through both rostrally projecting fibers and local interneuronal circuits. [71, 107, 108]. Our observations along with previous work to understand EES and track phrenic afferents suggest that CEES modulates respiratory activity through a sensorimotor circuit, likely dependent on SST-expressing interneurons in the layers I-IV of the dorsal horn. EES at lumbar levels preferentially activates sensory neurons leading to monosynaptic and polysynaptic

interneuron activation of motor neurons [109-111], and similar polysynaptic circuits in the cervical spine may be activated by CEES to enhance diaphragm activity. Similar to phrenic nerve stimulation, we found neuronal activation, as visualized by c-Fos immunofluorescence, in the dorsal horn, specifically lamina I-IV [112]. Phrenic afferent stimulation increases respiratory activity in cats and dogs [73, 107, 113]. Interestingly, Yu *et al*. found respiratory increases were inverse to anesthesia plane, and we observed a similar relationship in CEES in rats (D.C. Lu, unpublished observations). [73]. Nair *et al*. suggested that type III and IV phrenic afferents tend to increase respiratory activity while type I and II afferents have a more variable effect on respiratory behavior [108]. There is minimal evidence of monosynaptic connections between phrenic afferents and phrenic motor neurons, but the afferents project to spinal interneurons in several different lamina of the spinal cord [74, 108, 114]. Nair *et al*. found afferent projections in lamina I-IV as well as VII and X [74]. PRV-152 and c-Fos expression were observed following CEES in similar locations to the afferent projections reported by Nair *et al.* Moreover, PRV-152 was injected into the diaphragm and allowed to incubate for 64 hours allowing for multiple synaptic jumps, which likely labeled interneurons also receiving projections from afferents and motor neurons innervating the diaphragm [67].

SST expression in the spinal cord is mainly localized to the dorsal horn, mostly in lamina I-III and to a lesser extent lamina 4-5 [115, 116]. The majority of SST-expressing interneurons in the dorsal spinal cord are excitatory and receive input from Aβ, Aδ and C fibers and transmit mechano-sensation and nociceptive information [115-119]. In our experiments, inhibition of SST-expressing neurons in the cervical spine diminished CEES-induced respiratory activation (Figure 5). SST interneuron activation elicited by CEES is likely enhancing an excitatory spinal polysynaptic sensorimotor circuit through other interneurons in the spinal cord, which then influences phrenic motor neuron excitability making them more easily depolarized and activated by the descending central pattern generator activity. Consistent with such a hypothesis, we observed increased tonic diaphragmatic activity between inspiratory phases. In future work, we may explore the generality of such an effect by examining non-respiratory EMG activity in muscles whose nerves are of cranial origin (genioglossus), cervical and thoracic origin to non-respiratory or respiratory muscles (C3-

5, deltoid; T1-10, intercostal). Enhanced tonic activity in the deltoid without an increase in the genioglossus would support interneuron enhancing motor neuron excitability without an effect on the rostral brainstem respiratory central pattern generators. Additionally, enhanced tonic activity in caudal muscles might suggest a propriospinal influence of CEES.

The modulatory effect on respiratory activity of CEES-elicited afferent activity is likely derived from both spinal and supraspinal actions. Lamina II-IV, areas in which we found higher c-Fos positive cells in animals receiving stimulation, are known to receive and send information from primary sensory afferents to higher brain structures and local spinal interneurons (Figure 3) [120-122]. Additionally, experiments on the gate theory of pain suggest that neurons in lamina III provide polysynaptically projections to neurons in lamina I where projections ascend to higher brain structures [123, 124]. CEES is likely also activating sensory fibers traveling via the fasciculus cuneatus, sending information to the medulla, thalamus, and primary somatosensory cortex all of which can influence respiratory activity [75, 76, 112, 125]. The pons and medulla are the primary sites containing nuclei known to generate and control the respiratory pattern and to provide descending propriospinal premotor connections to phrenic motor neurons in the cervical spinal cord as well as, cranial and more caudal spinal motor neurons that innervate a wide variety of respiratory muscles [126-128]. Given the minimal hM4D(Gi) expression observed in the brainstem, the diminished respiratory modulation by CEES via inhibition of SST-expressing neurons in the spinal cord is a local phenomenon (Supplementary Figure 3). However, this set of experiments does not rule out the possibility of supraspinal structures contributing to CEES-induced respiratory modulation, instead it describes spinal circuit activation that is a more accessible site for neuromodulation throughout a physiologically meaningful sensorimotor system. Activation of this spinal sensory circuit by CEES, is likely to increase the activity of the ponto-medullary circuit so that in addition to sensitizing spinal motor neurons to descending inputs by intra-spinal mechanisms (as outlined above), CEES may also increase the overall drive to breathe so that the level of excitatory inputs to phrenic motor neurons and other spinal and cranial motor neurons innervating respiratory muscles is amplified.

While the dorsal horn SST neurons are mostly excitatory, there is evidence that SST neurons in deeper lamina can express inhibitory neurotransmitters suggesting the SST neurons in the spinal cord are heterogenous [116]. An inhibitory circuit that could explain the results that we found would require inhibition of an inhibitory respiratory inputs so that facilitation of respiratory activity could emerge. Inhibitory influences have been shown to influence phrenic nerve output both from supraspinal sources and local processes potentially originating from Renshaw cells [64, 84, 129, 130]. Further understanding of the circuit leading to enhanced respiratory activity from CEES can contribute to development of novel uses of CEES for use in spinal cord injury, traumatic brain injury, and stroke.

Typically, chemogenetic studies involving the expression of Cre under a promoter have been performed in mice. Since rats have been used in many respiratory studies; there is a well-developed literature describing respiratory control; they are larger and easier to handle; we explored EES modulation and chemogenetic inhibition approaches in wild-type rats. We used a novel dual viral vector strategy to perform chemogenetic experiments in rats that bypasses the difficulty and financial burden of breeding multiple generations of double- or triple-transgenic mice to express promoter specific Cre and DREADDs in a target neuronal population. Injection of both of the necessary cassettes using adenoviral vectors to achieve promotor-specific expression of the DREADD protein allows more flexibility when designing and performing experiments to understand neuronal circuits in rats. Broad expression of hM4D(Gi) in SST-expressing neurons reaching into brainstem respiratory generating nuclei allowed us to explore the involvement of SST-expressing neurons in CEES-induced respiratory modulation. This expression of hM4D(Gi) outside the cervical spine was minimal, and we conclude, therefore, that CEES-induced respiratory activation originates in the cervical spinal cord due to excitation of SST-expressing neurons. Alternatively, non-specific expression of hM4D(Gi) in neurons other than SST-expressing is possible. We explored this possibility as well and found an abundance of hM4D(Gi), as visualized with mCherry, co-localized with SST-expressing neurons identified through standard immunofluorescence techniques and minimal evidence of hM4D(Gi) expression outside of the regions expressing SST. Finally, high doses of

CNO has been shown to affect baseline behavior without expression of a DREADD receptor [131-133]. We used a low dose of CNO to mitigate this effect, and we controlled for this possibility by including a group of animals (AAV-SST-eGFP+AAV-hM4D(Gi)+CNO) that received viral constructs that did not result in the expression of the hM4D(Gi) receptor, as well as injections with CNO. We found respiratory behavior elicited by CEES similar to that seen in the baseline condition across the experiment suggesting that our results cannot be explained by CNO off-target affects.

We conclude that dorsal CEES activates a spinal sensorimotor circuit which can be used to enhance respiratory activity. Differences in modulation along the cervical spine could provide a useful tool to personalize the respiratory enhancement to an individual's specific deficit. In these experiments, we found a more rostral frequency modulation and caudal minute volume modulation. Comparing between sites did not show any one location was more efficient in modulation however, comparisons within each location revealed significant frequency increases at rostral levels while significant minute volume increases without frequency modulation was prevalent when CEES was applied at caudal levels. Future work to further dissect this respiratory sensorimotor circuit activation can provide a novel understanding of the spinal respiratory circuit and how brainstem nuclei are involved. Additionally, pre-clinical experiments in models of disease can provide a framework for CEES and its use to maintain spontaneous respiratory activity in cases of diminished respiratory activity.

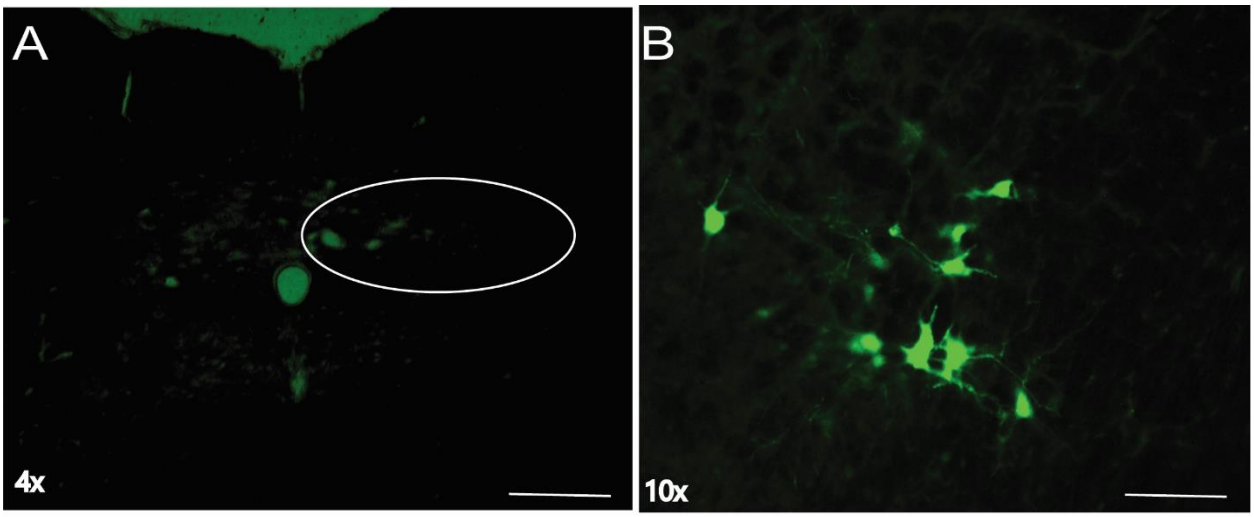

Supplementary Figure 2.1: A) Dorsal motor nucleus (DMN, circled above) was visualized in animals recieving PRV-152 injections into the diaphragm to ensure virus did not leak into the abdominal cavity. Slice is ~ -13.8 mm Bregma. Image taken at 4x. Scale bar is 330 uM. B) PRV-152 labled neurons in the ventrolateral medulla was visualized to ensure pre-motor neuron infection. Slice is ~ -13.8 Bregma. Image taken at 10x. Scale bar is 130 uM. CC-Central Canal

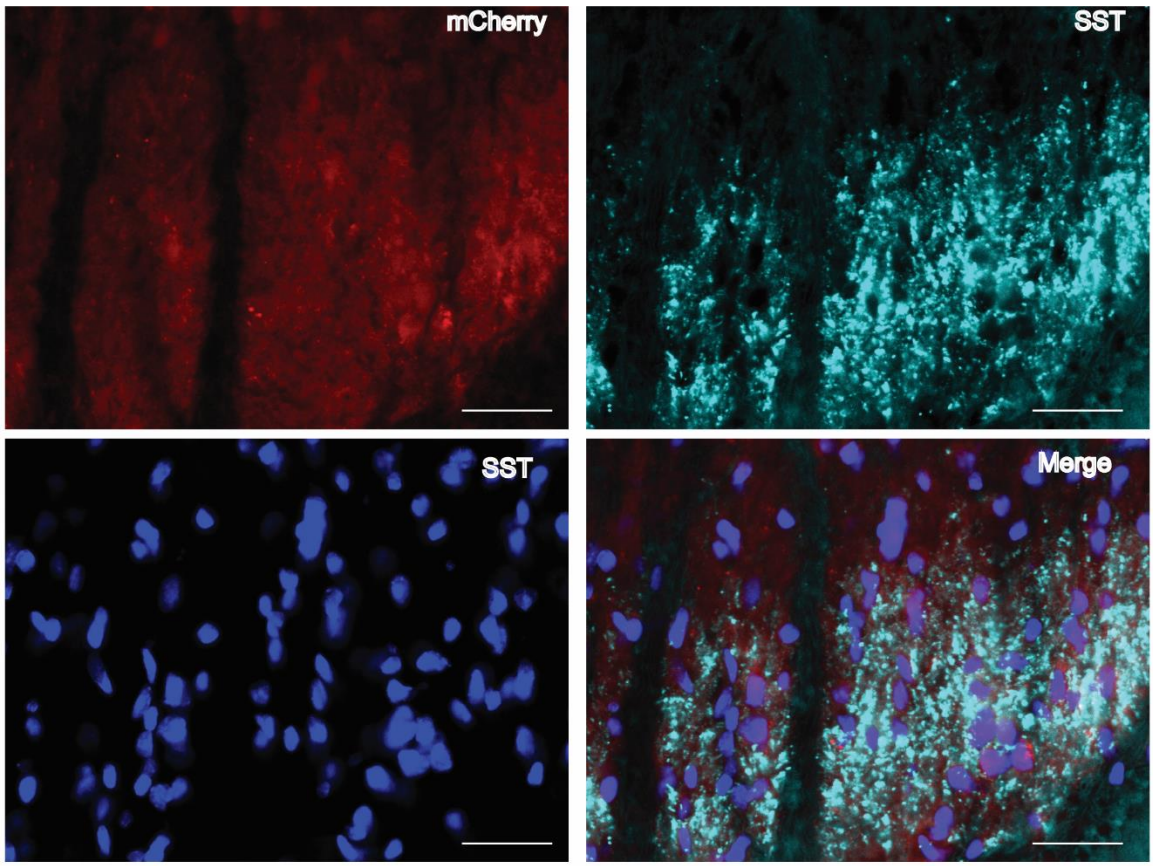

Supplementary Figure 2.2: mCherry expression of hM4D(Gi) co-localized with SST antibody in the dorsal horn. Images were captured at 40x. Scale bar is 30 um.

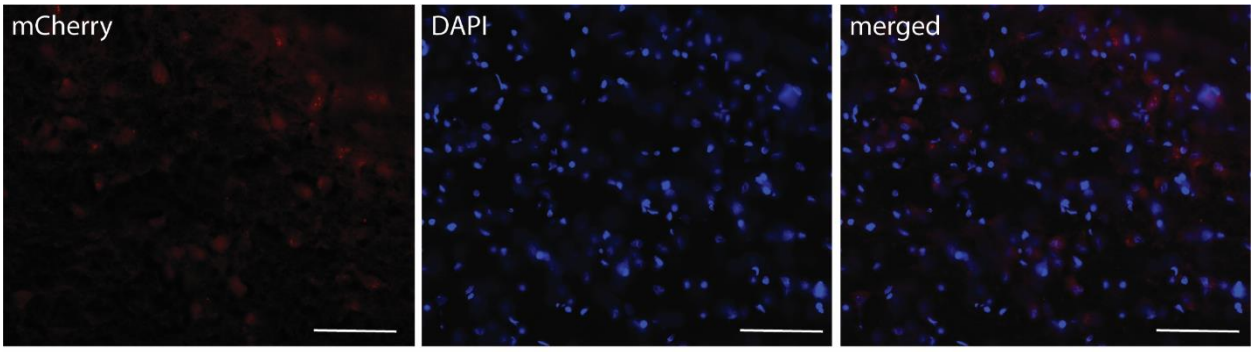

Supplementary Figure 2.3: Minimal mCherry expression in caudal brainstem rostral ventral respiratory group was observed after intraspinal injections of hM4D(Gi) in the cervical spinal. Images taken at ~ -13.8 mm. Bregma with 20x magnification. Scale bar is 70 um.

Chapter 3

Introduction

Traumatic spinal cord injury is a devastating event that damages descending neuronal connections from the brain to the spinal cord. It often results in paralysis below the level of injury. More than half of all spinal cord injuries occur to the cervical level [134]. Any injury to the cervical spinal cord, resulting in paralysis, causes respiratory deficits. These deficits can be as extensive as to necessitate chronic or periods of mechanical ventilation [135, 136]. While mechanical ventilation has proved useful to maintain respiratory needs, it has its own negative side effects such as lung injury and diaphragm atrophy [137-141]. Alternatively, individuals may retain spontaneous respiratory activity but have deficits in other respiratory behaviors like, coughing for airway clearance [136]. With higher rates of survival from traumatic injuries, new technologies to assist in ventilation and neurorehabilitation are needed.

Several forms of neuromodulation for respiratory function after spinal cord injury have been explored. Phrenic nerve pacing is one such technique that directly stimulates the nerve resulting in diaphragm activity [99, 142]. Yet, this approach restricts respiratory activity to a fixed rhythm and volume that lacks the fluctuations that naturally occur with respiration [143]. Additionally, the surgical technique for implantation is complicated and the risk of injury to the phrenic nerve is high [99]. Paced ventral stimulation of the thoracic or cervical spinal cord has shown beneficial results in pre-clinical animal models [102, 144, 145]. Intraspinal stimulation is another approach that activates respiratory muscles through stimulation of spinal inter- and propriospinal neurons [146, 147]. The surgical technique required to reach the ventral surface is difficult and invasive. Additionally, most of these studies have utilized paced stimulation which still restricts the variability observed during spontaneous respiration [145].

Dorsal epidural electrical stimulation (EES) is a technique that is FDA-approved for use in chronic pain conditions [148]. Implantations of the devices are routine for neurosurgeons. More recently, it has been shown to improve coordinated lower and upper extremity function after spinal cord injury when

combined with neurorehabilitation in both rodent models and clinical research studies [105, 149-152]. Since dorsal cervical EES (CEES) increases respiratory activity in intact anesthetized rats and mice, we sought to investigate if it can recover or enhance respiratory activity after cervical spinal cord injury through activation of spinal respiratory circuits [92, 153].

To explore if CEES can enhance respiratory activity after a high cervical spinal cord lesion, animals received a lateral C2 hemisection, which severs dominant bulbospinal respiratory projections, resulting in ipsilateral diaphragm paralysis. Multiple bouts of CEES were performed to explore recovery of respiratory muscle activity and enhancement of respiratory activity. Rhythmic ipsilateral diaphragm bursting was observed during and after stimulation. Injury area was compared to CEES-induced diaphragm activity to determine the contribution of spared projections to the recovery of diaphragm activity. Finally, we explored spinal inhibitory influence reducing the effectiveness of CEES on respiratory muscle activity [103]. The results of these experiments suggest CEES could be a useful therapeutic in the acute period after spinal cord injury to enhance diaphragm function and potentially minimize need for mechanical ventilation.

Materials and Methods

Female Sprague-Dawley rats (270-300 g, n=31) were ordered from Envigo and were allowed to acclimate for one week. Animals were kept in a 12-12 light-dark cycle with *ad libitum* standard food and water. All procedures were approved by the University of California Animal Research Committee (protocol # 2014-122) and were in accordance with the Guide for the Care and Use of Laboratory Animals of the National Institutes of Health.

Surgical Procedures

Rats were prepared for a non-survival surgery with intraperitoneal injections of urethane (1200 mg/kg) and alpha-chloralose (30 mg/kg) for anesthesia. Each rat was kept on a water-circulating heating pad to prevent hypothermia during the experiment. A tracheostomy was performed through a vertical incision

made ventrally on the neck and the sternohyoid muscles were separated to expose the trachea. A small incision was made between the cartilage rings of the trachea and a short segment of PE 200 tubing was inserted and connected to a pneumotach (Validyne, Northridge, CA) to record tracheal flow. An abdominal incision was performed to expose the diaphragm and two wires (St. Steel 7 Strand, AM-Systems, Sequim, WA), with the insulation stripped at the end (2 mm), were inserted bilaterally into the lateral costal portion of the diaphragm muscle for EMG recording. EMG signals were amplified 10^3, a bandpass filter, 300-1000 Hz, and a 60 Hz Notch filter applied. The animal was flipped prone and a laminectomy was performed to expose cervical levels 2 (C2) through 5 (C5) of the spinal cord.

Prior to the C2 hemisection, baseline EMG and ventilation values were recorded for at least 1 minute. A small incision was made into the dura overlying the rostral aspect of C2 spinal cord. Using micro scissors, a lateral incision was made into the spinal tissue from the posteriomedial vein to the lateral vertebra. A scalpel was then used to sever any remaining connections. Ipsilateral diaphragm EMG was confirmed absent at the end of the hemisection procedure. At this time, most animals were stable and did not require mechanical ventilation. A few animals necessitated a constant flow of O_2 to maintain unassisted eupnea (n=4). These animals were included in the experiment for EMG analysis but spontaneous respiratory ventilation values were not obtained. 45 minutes elapsed to allow for spinal shock to decrease and for physiological parameters to stabilize.

Epidural electrical stimulation

Animals underwent multiple trials of cervical epidural electrical stimulation (EES) or sham for 5 minutes. EES was delivered as a continuous 30 Hz monophasic (500 μs pulse width) train of impulses (Master 9 A.M.P.I., Jerusalem, ISR). The stimulating electrode (Tungesten Parylene 0.01", AM-Systems) was placed on the dorsal surface of the spine, ~2 mm from midline and the ground electrode was placed on the dorsal surface of the spine ~2-3 mm away from the stimulating electrode. The ends of the electrodes were stripped, leaving ~2 mm of the electrode tip uninsulated. Sham stimulation trials, in which electrodes were placed on the dorsal cervical spinal cord but no current was delivered, were performed to verify

mechanical pressure of the electrodes did not affect respiratory activity. Stimulation amplitudes ranged from 0.5-1.5 mA.

At the end of the experiments, animals were perfused transcardially with 1X PBS followed by 4% paraformaldehyde (pH 7.3). Tissue was extracted and post-fixed for 24 hours in 4% paraformaldehyde, placed in 30% sucrose for cryopreservation, and then placed into 10% gelatin and frozen.

Injury Area Assessment

Tissue was sectioned into 30 μm coronal slices using a cryostat (Leica CM 1800). Sections were stained with cresyl violet. Images of the spinal cord injury were taken to assess the completeness of the hemisection and examine any differences in response to CEES that may be explained by the injury area. Area of the injury was analyzed with ImageJ. The area of the contralateral side was outlined using the central canal and midline to distinguish ipsilateral and contralateral. Residual sparred tissue on the ipsilateral side was outlined to quantify extent of the injury. Healthy tissue presented as equal tone from staining and complete tissue presence. Injury area was observed as tissue absent, bloody with absent or light staining. Three slices at the injury site were used to quantify and obtain an average calculation of sparred tissue.

Pharmacological Inhibition

To investigate local spinal inhibition suppressing CEES induced diaphragm muscle activity enhancement, 1 mM Bicuculline and 1 mM Gabazine (GABA antagonists) or 1 mM Strychnine (glycine antagonist) were injected intraspinal. Animals (n=16) underwent the same procedures as described above. After initial CEES assessments after C2 hemisection were performed, animals received bilateral intraspinal injections of antagonists at the caudal end of C2. Intraspinal injections were performed using a micropressure injector (model) lowered to a depth of ~ 0.70 mm to target dorsal and intermedial interneurons. Injection volumes were 250 nL delivered at a rate of 2 nL/sec. 10 minutes passed before the injection needle was withdrawn from the spinal cord after each injection. Another 10 minutes elapsed

after withdrawal of the needle for antagonist to have effects. Stimulation trials began 20 minutes after the last intraspinal injection and continued for at least an hour after the injection.

Data Analysis

A hemisection was considered complete when ipsilateral rhythmic activity was no longer observed. Respiratory and EMG data was acquired with DataView (W.J. Heitler, University of St. Andrews). Data extraction and analysis were performed with custom Matlab codes. Prism was used for statistics and data visualization.

A probability score of rhythmic bursting in the ipsilateral diaphragm was obtained by splitting the 300 s of stimulation into 10 sets of 30 s analysis windows. If an animal had rhythmic bursting during that time the animal received a 1, if no bursting was observed the score was 0. The average score for an animal was obtained by averaging the score across all possible analysis windows. A mixed effects model in which condition (Stim/Sham/Post-Stim/Post-Sham) was a within subject factor was applied to the probability data. The rhythmic activity observed during the analysis windows was analyzed as the average integral of the envelope obtained from the EMG data. EMG data was bandpass filtered (30 Hz), rectified, and a 5^{th} order Butterworth filter applied to obtain the area under the curve. Stimulation obscured the EMG signal in most animals which hindered analysis of bursting activity during stimulation. The intra EMG data was taken when stimulation signal did not obstruct rhythmic diaphragm activity or when the stimulation probe was briefly removed from the dura. Ipsilateral diaphragm activity was considered rhythmic when bursting was in sync with contralateral diaphragm activity. The average time window of EMG signal used for analysis during stimulation was 59 seconds and ranged from 8-153 seconds. Out of 15 animals, 1 never responded with rhythmic ipsilateral bursting activity that could be extracted. EMG data was analyzed with a one-way repeated measure ANOVA (Intra) or a paired T-test (Post).

Tidal volumes were calculated from the integral of the inspiratory flow. Respiratory data was analyzed with a mixed effects model with treatment (Stim/Sham) a within subjects factor and Time (serial measurements) a within subjects factor. Residual ipsilateral tissue at the site of injury was compared to

the average EMG integral during stimulation. EMG integral comparisons of CEES and CEES with inhibitory antagonists was analyzed with a mixed effects model where condition was a within subjects factor. A Bonferonni correction was applied to account for multiple comparisons.

Results

To investigate CEES as a method to increase respiratory activity after a respiratory compromising injury, CEES was applied to the dorsal C3 spinal cord 45 minutes after a C2 hemisection. Rhythmic ipsilateral diaphragm activity was observed during CEES, Figure 1B. There was a significant effect of condition when the probability of rhythmic bursting was analyzed ($F_{(1.915, 21.06)} = 13.74$, df = 4, p = 0.0002). CEES significantly increased the probability that rhythmic ipsilateral diaphragm activity occurred compared to during Sham (Stim 0.53 ± 0.39, Sham 0.09 ± 0.20, p = 0.007), Figure 1C. We quantified the diaphragm burst activity activated by CEES or Sham and found a significant effect of condition ($F_{(2, 35)} = 16.77$, df = 37, p = 0.0001). The average ipsilateral EMG burst integral (4231.3 ± 4292.0) was significantly greater than sham trials (333 ± 500.1, p = 0.039), Figure 1D. Ipsilateral EMG burst integral however, remained significantly lower than baseline activity (Pre 7859.3 ± 3584.5, p = 0.013).

After stimulation ended, the probability of rhythmic bursting decreased (0.26 ± 0.29) but was observed in most animals, Figure 1C. The burst integral of diaphragm activity after stimulation ended also decreased and was not significantly different from sham values (Stim 1788.2 ± 1484.2, Sham 690.8 ± 1697.3, p = 0.09), Figure 2C. However, the time duration of rhythmic bursting in the paralyzed diaphragm was significantly longer after Stim (Post-Stim 95.4 sec ± 88.5 sec) trials compared to Sham (Post-Sham 25.8 sec ± 71.0 sec, p = 0.024) trials, Figure 2D. These results suggest CEES can enhance rhythmic activity in paralyzed respiratory muscle after a C2 hemisection and slowly returns to near baseline levels after stimulation ceases.

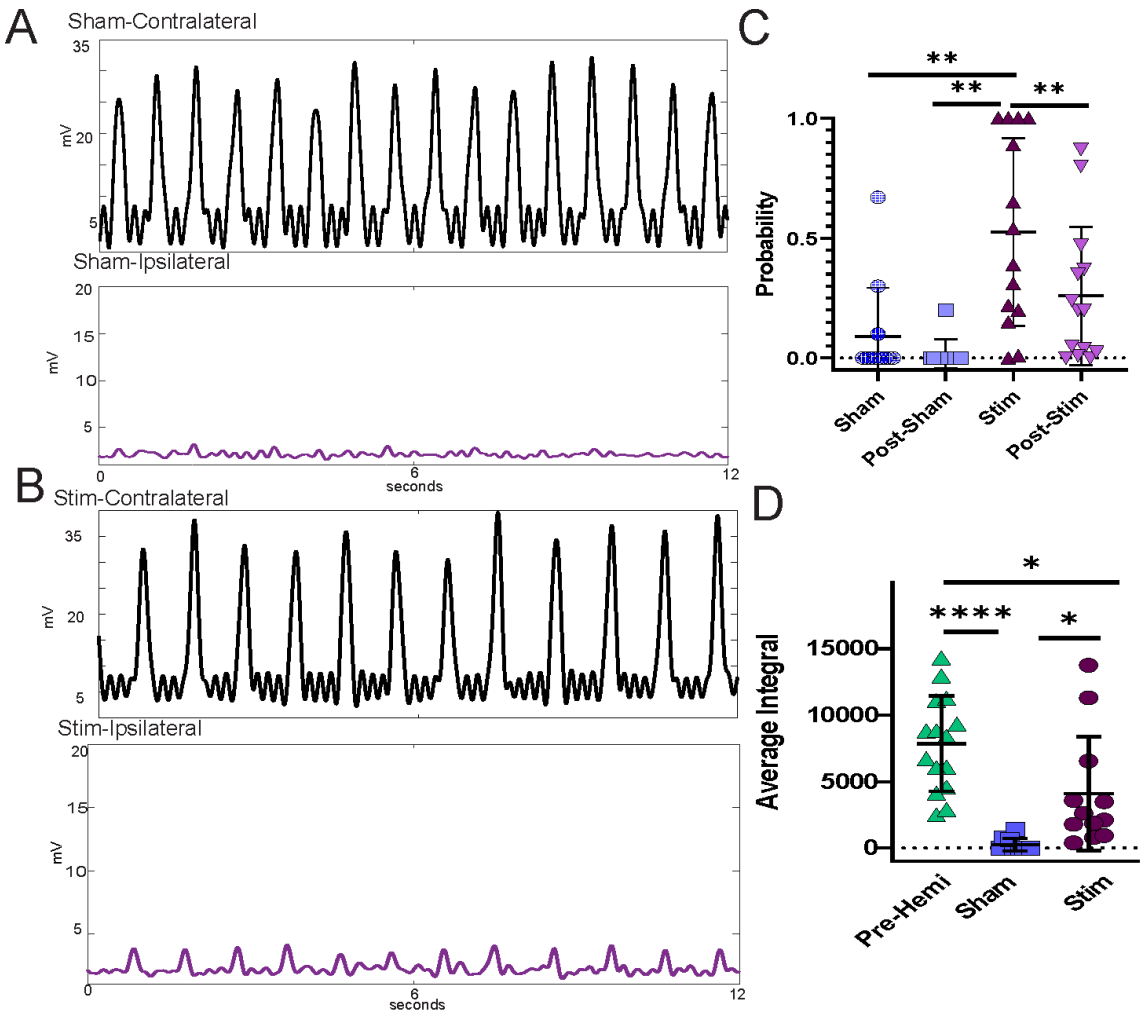

Figure 3.1: Epidural electrical stimulation activates ipsilateral diaphragm activity in the acute period after C2 hemisection. A) Representative trace showing the envelope of contralateral and ipsilateral diaphragm activity during sham trials. B) Represenative trace showing envelope of contralateral and ipsilateral diaphragm activity during 30 Hz CEES. C) CEES significantly increased the probability of rhythmic bursting in the ipsilateral diaphragm compared to sham trials. D) CEES significantly increased diaphragm activity when bursting was observed. Probability of bursting data was analyzed with a mixed effects model with condition (Sham, Stim) a between subjects factor and time a within subjects factor. Bonferonni correction was applied to account for multiple comparisons. Rhythmic bursting activity was analyzed with a one-way ANOVA and Bonferonni correction applied for multiple compari-sons. n=15

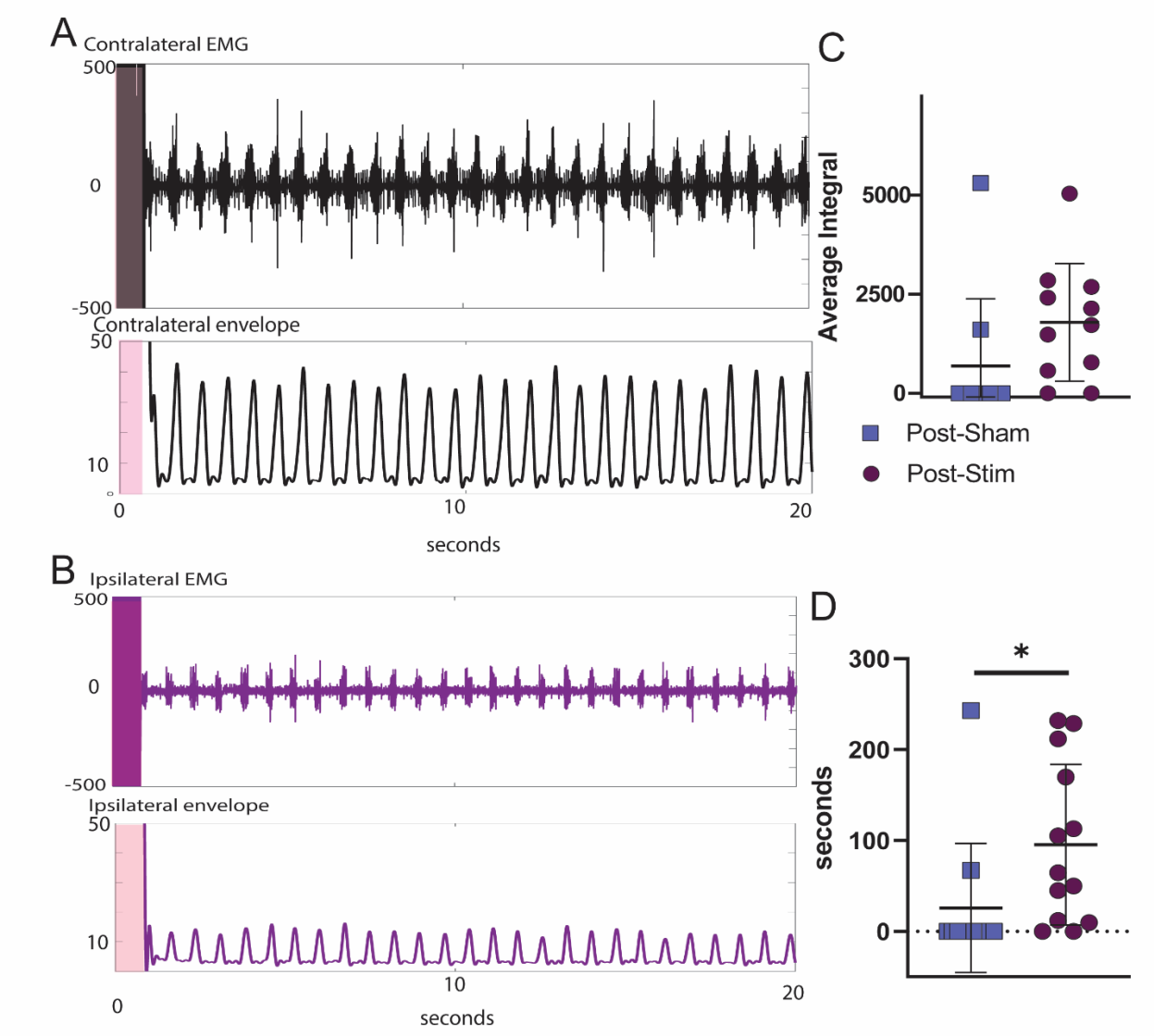

Figure 3.2: Rhythmic ipsilateral diaphragm bursting was observed for some period of time after CEES. A) Contralateral diaphragm activity (top) and envelope (bottom) of the rhythmic bursting activity. B) Ipsilateral diaphragm activity (top) and envelope (bottom) of the rhythmic bursting activity after CEES ended. C) Quantified average rhythmic bursting activity observed in ipsilateral diaphragm after CEES. D) Average time rhythmic bursting was observed in the diaphragm after CEES. Activity and rhythmic bursting time was analyzed with a paired T-test. n=15

To assess functionality of CEES induced diaphragm activity frequency, tidal volume, and minute volume were assessed prior to, during, and after CEES. There was a significant interaction of condition and time for respiratory rate ($F_{(2, 14)} = 4.59$, df = 2, p = 0.029). However, respiratory frequency during stimulation was not significantly different from baseline (Pre 73.1 BPM ±16.0 BPM, Intra 69.5 BPM ± 15.1 BPM, p >0.05), Figure 3B. There was a significant interaction of condition and time for respiratory tidal volume

($F_{(2, 14)}$ = 7.40, df = 2, p = 0.006). Tidal volume was significantly increased during CEES (Intra .27 mL ± 0.27 mL) compared to baseline (Pre 0.22 mL ± 0.23 mL, p = 0.013) periods, Figure 3C. This increase in tidal volume did not persist after CEES ended (Post 0.23 mL ± 0.24 mL, p = 0.22). There was no significant interaction for minute volume between condition and time, Figure 3D. Contralateral EMG before, during, and after CEES was quantified to account for diaphragm activity receiving direct bulbospinal input, Supplementary Figure 1. No interaction or differences were observed in the contralateral diaphragm EMG activity across the different time points analyzed (p>0.05). This data suggests that in the acute time period, CEES increases spinal respiratory activity resulting in ipsilateral diaphragm activity that contributes to increased respiratory tidal volume.

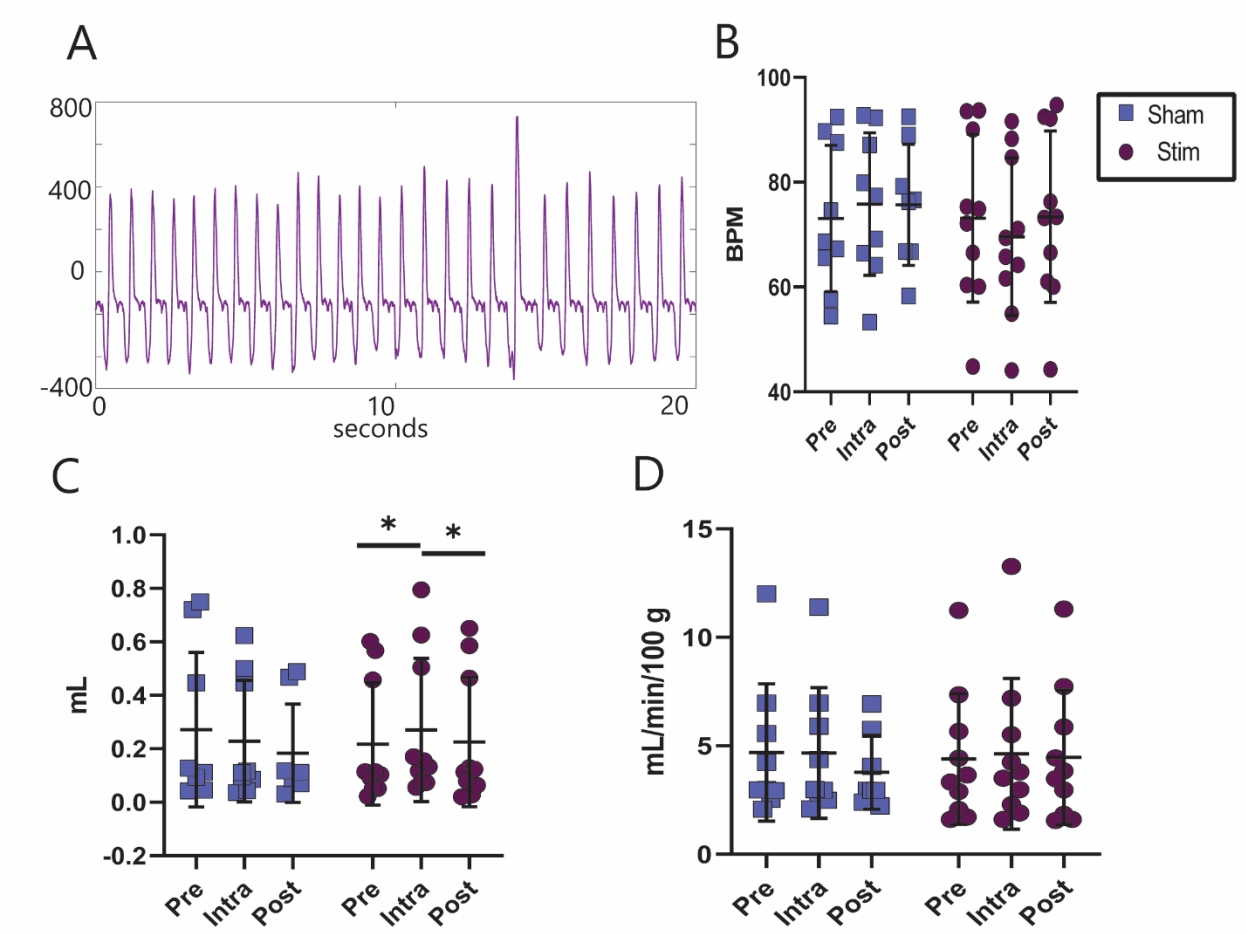

Figure 3.3: Respiratory tidal volume increased during stimulation. A) An example of respiratory activity during CEES. B) Respiratory frequency remained unchanged during CEES. C) Tidal volume was significantly increased during CEES and returned to baseline after stimulation. D) Minute volume remained unchanged during stimulation. Data was analyzed with mixed effects model with Sham vs Stim a between subjects factor and time a within subjects factor. n=15

We explored the injury with the idea that the severity of injury or spared tissue may lead to some understanding about the extent to which CEES enhanced diaphragm activity, Figure 4. Contrary to our hypothesis, injuries with a smaller area of spared tissue did not predict a poor response to CEES, Figure 4B. This suggests local ipsilateral and contralateral spinal circuits are being activated to enhance respiratory activity during CEES.

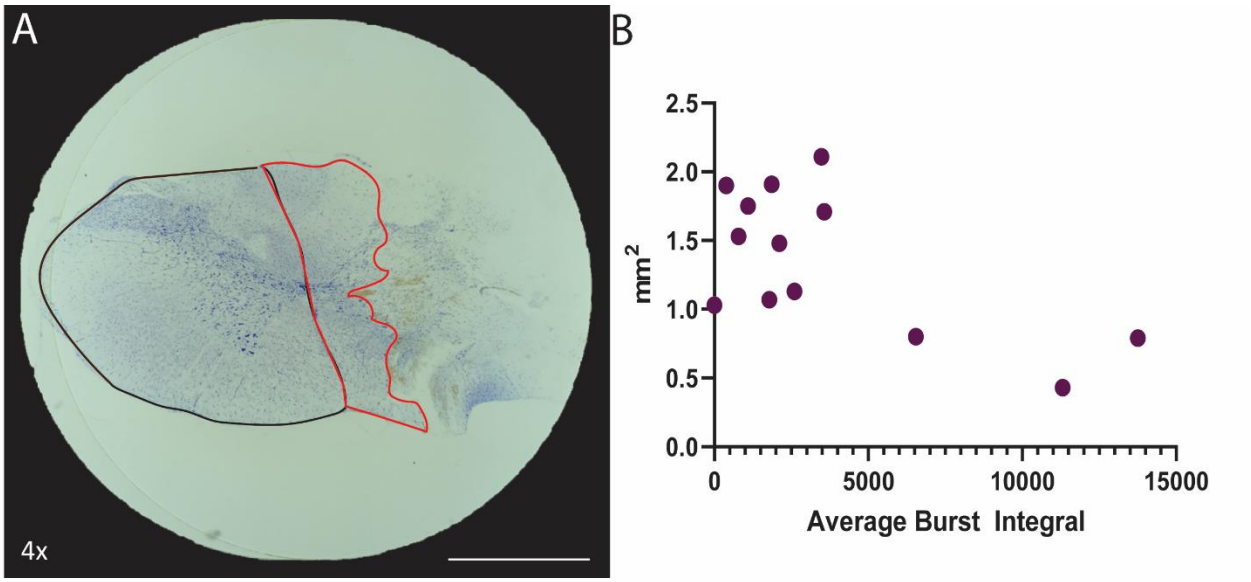

Figure 3.4: Area of spared tissue compared to CEES induced diaphragm bursting size A) Representative figure showing a 4x image of the C2 spinal cord level and the contralateral (outlined in black) and sparred ipsilateral (outlined in red) tissue areas measured with ImageJ. B) The area of sparred spinal cord tissue on the ipsilateral side to the C2 hemisection did no predict magnitude of ipsilateral diaphragm bursting during CEES. scale bar = 930 um

Local spinal inhibitory neurostransmitters, GABA and glycine, are known to reduce spinal respiratory motor neuron activity and inhibition of their influence has been shown to enhance spontaneous phrenic nerve activity after C2 hemisection [47, 154-156]. We hypothesized spinal inhibition may hinder the effects CEES has on paralyzed muscle activity after hemisection. However, we found no evidence that CEES initiated ipsilateral diaphragm activity was enhanced after 1 mM bicuculline and 1 mM gabazine or 1 mM strychnine microinjection, as shown in Figure 5.

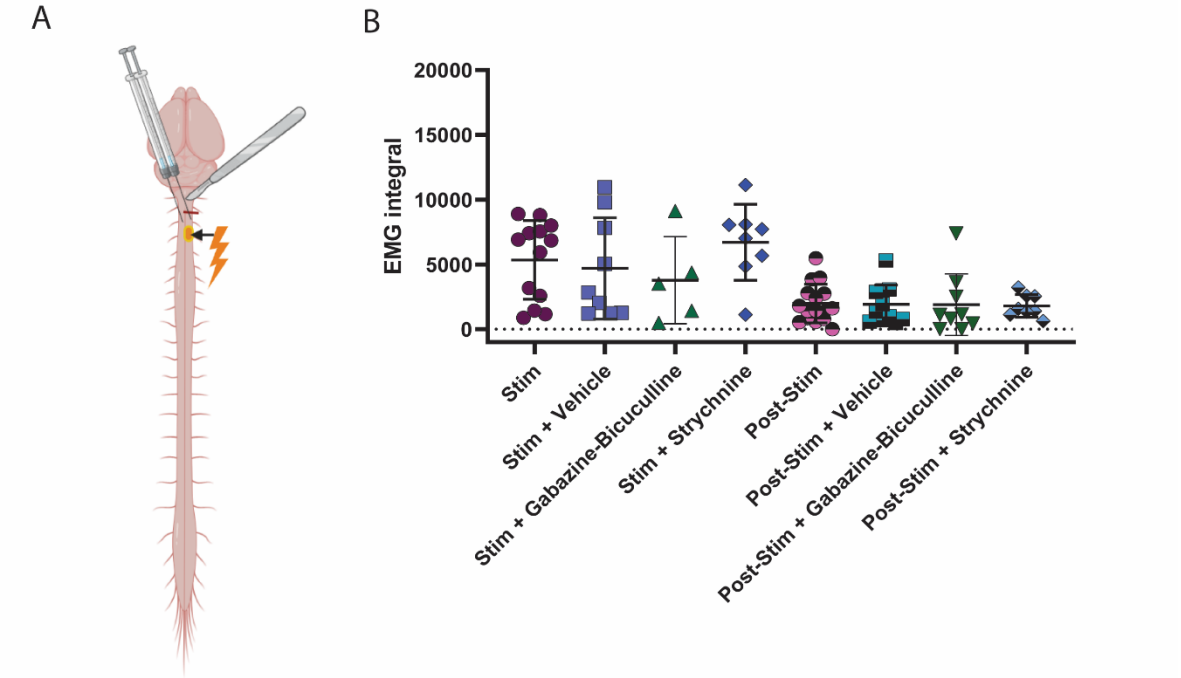

Figure 3.5: Local blockade of fast inhibitory neurotransmission does not enhance CEES induced ipsilateral diaphragm activity. A) Experimental set-up in which the animal received a C2 hemisection, bilateral microinjection of 1 mM Gabazine/Bicuculline or 1 mM Strychnine, and CEES at C3. B) Average diaphragm bursting activity prior to drug deliver, after vehicle (DMSO or saline), and after drug treatment. Data was analayzed with a mixed effects model with treatment as a within subjects factor. n=8 Gabazine-Bicuculline, n=8 Strychnine. Image made with BioRender.com.

Discussion

In this study, CEES to enhance respiratory activity after a C2 hemisection was explored. CEES significantly increased the probability of ipsilateral diaphragm activity during stimulation compared to sham trials. The diaphragm activity that occurred with stimulation was significantly increased compared to sham trials. When CEES ended, the probability of bursting and the activity observed decreased. However, the amount of time rhythmic activity was observed in the ipsilateral diaphragm was significantly longer compared to post-sham periods. Tidal volume was significantly increased during CEES compared to baseline. Contralateral EMG before, during, and after CEES was quantified and found to be similar across all time points analyzed. These results suggest, CEES can activate a spinal respiratory circuit that can initiate activity in paralyzed diaphragm muscle, and this activity contributes to increases in

tidal volume. Area of tissue spared from the hemisection was compared to the ipsilateral EMG initiated by CEES. There was no correlation between spared tissue area and outcome, suggesting residual descending projections were not the primary source of activation for rhythmic ipsilateral diaphragm activity. Spinal inhibitory activity minimizing beneficial effects of CEES was explored using intraspinal injections of GABA (Bicuculline/Gabazine) or glycine (Strychnine) antagonists. In this set of experiments, local blockade of fast inhibitory neurotransmitters did not enhance EES induced respiratory activity.

CEES has shown to increase respiratory activity in anesthetized rats and mice, likely through activation of spinal sensory interneurons and brainstem nuclei [92, 153]. We hypothesized that cervical CEES would enhance spinal respiratory circuits leading to enhanced diaphragm activity after high cervical spinal cord injury. While we observed rhythmic bursting in paralyzed diaphragm muscle at the acute time point, the bursting often slowly decreased with time after stimulation. However, chronic stimulation may prove beneficial through mechanisms similar to activity dependent plasticity. Activity dependent plasticity has several known mechanisms leading to strengthening of new or latent synaptic circuits resulting in new behavioral outcomes. BDNF, a known neurotropic signaling molecule, has roles in plasticity, learning and memory, and motor function after spinal injury [157, 158]. It has been shown to be decreased after spinal cord transection and EES can increase its expression [159]. NMDA and AMPA receptor activity are well known for their role in long-term potentiation and synaptic strengthening within sensorimotor circuits [160, 161]. Interestingly, strengthened connections between motor and sensory neurons is dependent on NMDA activation [161, 162]. Since EES is known to activate sensory circuits, it is possible long-term EES could enhance diaphragm activity through sensorimotor circuit strengthening via NMDA receptors. With the observation that EES induces rhythmic activity in paralyzed diaphragm after spinal lesion, chronic use of CEES and its effects on neural circuit plasticity should be explored.

Strengthening of latent synaptic circuits with CEES could lead to plasticity and enhanced respiratory activity over the long term through strengthened spinal interneuronal circuits. Chemical and

pharmacological methods to enhance respiratory drive have been shown to induce diaphragm activity in the paralyzed muscle after high cervical spinal cord injury [163-165]. Chronic intermittent hypoxia activates ipsilateral diaphragm activity after hemisection and strengthens connections among cervical excitatory interneurons [166, 167]. Furthermore, cervical excitatory interneurons have been shown to maintain and activate rhythmic phrenic activity in the absence of direct bulbospinal input [65, 80, 168] Yet, this is an important exploration as the authors have no reason to believe CEES induced diaphragm activity is mechanistically similar to intermittent hypoxia-induced respiratory plasticity.

Ventrolateral spinal epidural stimulation has recently been shown to activate rhythmic phrenic nerve activity in the C2 hemisection model at the sub-acute and chronic time point when applied "across the respiratory cycle" [144]. At the chronic time-point, the ventrolateral stimulation potentiated phasic activity more than what was observed at the sub-acute time point. If similar interneuronal circuits are being activated with the dorsal approach as used in this experiment, CEES at sub-acute and chronic time points after injury may be beneficial as a respiratory therapeutic. However, experiments stimulating on the ventral surface have primarily used high-frequency stimulation protocols and differential responses to stimulation have been observed when different frequencies are utilized [106]. More recently, high frequency stimulation applied to the dorsal epidural surface has been shown to pace diaphragm muscle activity after C2 hemisection [103]. We suggest pacing is an ineffective form of neurorehabilitation but may be useful for neuroprosthetics if plasticity and neurorehabilitation are beyond possibility due to injury severity. Alternatively, pacing strategies coupled with our constant low-amplitude stimulation strategy could couple local excitatory respiratory drive and motor output to enhance respiratory output. Our results exemplify the ability of the spinal respiratory circuits to utilize dormant pathways to activate spontaneous rhythmic activity likely through spinal sensorimotor circuit when activated by cervical CEES [153]. Further exploration on frequency specific responses by neurorehabilitative therapeutics on the spinal cord and circuit modulation could provide a broader range of benefits.

Inhibitory activity is known to inhibit spinal respiratory circuits in the absence of direct bulbospinal activity [47, 80, 155]. We explored if this inhibition had any restrictive effect on the ability of CEES to enhance diaphragm motor output in the paralyzed diaphragm. CEES induced rhythmic diaphragm activity was not enhanced when GABA or Glycine fast neurotransmission was inhibited. This result is similar to what others have observed with epidural stimulation diaphragm enhancement [103]. We propose that the respiratory timing is dependent on local inhibitor and excitatory balance but initiation of dormant pathways with CEES is not enhanced by reducing fast inhibitory activity.

The C2 hemisection model is used in research to imitate respiratory deficits from cervical spinal cord injury resulting in ipsilateral diaphragm paralysis for several weeks [169-171]. A plethora of knowledge has been obtained on spontaneous and induced plasticity and its mechanisms relating to respiratory activity [144, 165, 167, 169, 172, 173]. While its use in research has provided scientists with a standardized model to explore plasticity with tangible outcomes, it is important to mention this model is not well suited to model the traumatic spinal cord injury humans often experience. And spontaneous recovery is more substantial in the weeks after hemisection when examined in awake freely moving animals compared to anesthetized experiments [170]. Additionally, we as well as others have found that spared ipsilateral tissue is often observed despite paralysis of the ipsilateral diaphragm [170]. This tissue sparing may contribute to CEES evoked ipsilateral diaphragm activity and potential plasticity (similar to that seen in humans) in the neural networks leading to better respiratory outcomes [174, 175]. However, in this experiment, we found no correlation to suggest that more spared tissue resulted in more activity in the ipsilateral diaphragm during CEES.

We conclude that CEES can activate spinal circuits leading to diaphragm activity in paralyzed muscle that can increase tidal volume in the immediate time after a C2 hemisection in anesthetized rats. CEES at the sub-acute (days) and chronic (weeks/months) period after hemisection should be further explored.

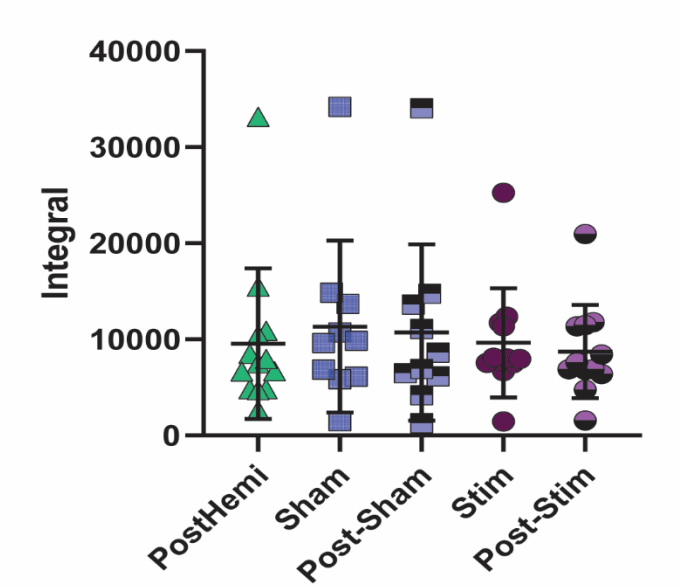

Supplementary Figure 3.1: Contralateral diaphragm EMG envelope was analyzed across time and conditions to explore how EES applied ipsilateral and caudal to C2 hemisection affected diaphragm activity on the contralateral side. There was no significant difference between conditions and time $p>0.05$. Data was analyzed with a mixed-effects model with condition (Sham, Stim) a fixed factor and subjects a random factor.

Chapter 4

The two previous chapters described novel experiments the author conceptualized, designed and executed to understand dorsal cervical EES (CEES)-induced increases in respiratory activity and its use in a model of cervical spinal cord injury with respiratory deficits. Experiments in Chapter 2 describe novel experiments exploring CEES modulation of respiratory activity. We found that CEES increases respiratory activity in anesthetized rats and that this effect is dependent upon activity in SST-expressing neurons in the spinal cord. This work suggests that EES at the cervical spinal cord can activate local and likely supraspinal respiratory circuits to influence respiratory rhythm and pattern generators and enhance respiratory activity. Chapter 3 described experiments aimed at exploring use of CEES in the early time after high cervical spinal cord injury. Application of CEES at the acute time period after a C2 hemisection activated paralyzed diaphragm activity in anesthetized rats. Blockade of local fast inhibitory neurotransmition did not enhance CEES-induced diaphragm activity. These results begin to describe a novel neuromodulation method for accessing respiratory neural circuits and enhancing respiratory activity. Continual exploration of these concepts can lead to improved clinical therapeutics and respiratory outcomes.

Experimental Pitfalls and Limitations

Several experimental limitations have been suggested throughout the previous chapters but a formal discussion is beneficial. In Chapter 2, c-Fos expression was used to identify neurons activated by CEES. C-Fos is an early expression gene whose protein (known as a transcription factor) has effects on downstream gene expression, and in turn modifies cellular activity [176]. The control animals that received PRV-152 and surgical preparation had minimal c-Fos activation. These data suggest that the majority of c-Fos expression observed in the experimental group was induced by CEES. However, describing the effects of this neuronal activation with specific cellular processes is not possible with these techniques alone.

Typically, chemogenetic studies involving the expression of Cre under a promoter have been performed in mice. Since rats have been used in many respiratory studies; there is a well-developed literature describing respiratory control; they are larger and easier to handle; we explored EES modulation and chemogenetic inhibition approaches in wild-type rats. We used a novel dual viral vector strategy to perform chemogenetic experiments in rats that bypasses the difficulty and financial burden of breeding multiple generations of double- or triple-transgenic mice to express promoter-specific Cre and DREADDs in a target neuronal population. Injection of both of the necessary cassettes using adenoviral vectors to achieve promotor-specific expression of the DREADD protein allows more flexibility when designing and performing experiments to understand neuronal circuits in rats. Broad expression of hM4D(Gi) in SST-expressing neurons reaching into brainstem respiratory-generating nuclei allowed us to explore the involvement of SST-expressing neurons in CEES-induced respiratory modulation. This expression of hM4D(Gi) outside the cervical spine was minimal, and we conclude, therefore, that CEES-induced respiratory activation originates in the cervical spinal cord due to excitation of SST-expressing neurons. Alternatively, non-specific expression of hM4D(Gi) in neurons other than SST-expressing is possible. We explored this possibility as well and found an abundance of hM4D(Gi), as visualized with mCherry, co-localized with SST-expressing neurons identified through standard immunofluorescence techniques and minimal evidence of hM4D(Gi) expression outside of the regions expressing SST. Finally, high doses of CNO affects baseline behavior without expression of a DREADD receptor [131-133]. We used a low dose of CNO to mitigate this effect, and controlled for this possibility by including a group of animals (AAV-SST-eGFP+AAV-hM4D(Gi)+CNO) that received viral constructs that did not result in the expression of the hM4D(Gi) receptor, as well as injections with CNO. We found respiratory behavior elicited by CEES similar to that seen in the baseline condition across the experiment suggesting that our results cannot be explained by CNO off-target effects.

Viral leakage causing non-respiratory neuron labeling is always possible, but this is unlikely to be a significant influence in these experiments since the dorsal motor nucleus was not labeled by the GFP

reporter of PRV-152 (Supplementary Figure 1A), and the PRV-152 label was restricted largely to the brainstem and nuclei with known respiratory activity. Mononuclear infiltration and glial immunoreactive cells have been observed when PRV-152, an attenuated strain of the herpetic pseudorabies virus, is left to replicate for long periods due to an immune response from the infection [67, 177]. These observations have mainly been published after incubation for 72 hours and longer [67, 177]. PRV-152 incubation was restricted to 64 hours in the current experiments to maximize polysynaptic transport and minimize immune cell infiltration. Additionally, the control animals showed minimal signs of c-Fos activity, indicating immune cells were not significantly contributing to c-Fos expression. Additionally, c-Fos expression was in both PRV-152 labeled and non PRV-152 labeled neurons in the animals that received active stimulation. It is possible that some of the cells expressing GFP were of glial origin as these cells pick up the debris from infected and lysed cells. However, this population of cells is likely low, and the expression similarly low due to use of the less virulent PRV and relatively shorter incubation times [178]. In addition, even if they picked up and expressed PRV-152 subsequent labeling of cells through synaptic transfer is unlikely as synaptic transfer from glial cells has not been observed [178].

The experiments in Chapter 2 consider mechanisms and relationships of spinal circuitry (high cervical spinal neurons) and brainstem networks (medullary circuits) to the increased respiratory drive. However, these experiments do not make any conclusions about the individual circuits in isolation. Instead, we have focused on understanding a sensorimotor respiratory circuit activated by CEES in a physiologically complete system. While understanding neuronal circuits in isolation expands scientific understanding, humans are an integrated system and rarely would one be completely isolated from supraspinal structures. An integrative approach to enhance supraspinal and spinal circuit activity can be useful to improve respiratory outcomes and potentially prevent use of long-term mechanical ventilation in a variety of conditions (stroke, traumatic spinal cord injury, traumatic brain injury, amyotrophic lateral sclerosis).

In Chapter 3, diaphragm EMG activity was the primary measurement of respiratory circuit activity. This measurement varies according to electrode location and inter-electrode distance. Baseline measurements

were made prior to hemisection and electrodes were not moved after the baseline measurements were made to control for this variable. EMG is a measure of motor neuron activity that results in muscle contraction and is recorded between the two electrodes. Therefore, this measurement only captures the activity of motor units innervating the muscle within the vicinity of the electrodes. It is possible that muscle activity in the ipsilateral diaphragm was under appreciated in the present experiments. Recording from the phrenic nerve would give a more accurate estimation of the total output generated to activate ipsilateral diaphragm activity. Nonetheless, robust activity was observed in CEES-induced diaphragm muscle after C2 hemisection.

Local spinal inhibition was explored to determine its effects on CEES induced diaphragm activity. Microinjection in volumes of 250 nL and 500 nL were performed caudal to the C2 hemisection and rostral to the site of stimulation (C3). These volumes are large compared to injection volumes used in the brain and other published methods in the spinal cord. Recently, pacing of phrenic nerve activity evoked through dorsal epidural stimulation using high-frequency stimulation similarly was unaffected by local spinal inhibition after C2 hemisection, supporting the data here [103].

Future Directions

It is the author's belief that the next step in this endeavor is to investigate EES in the sub-acute phase (days to weeks) after spinal cord injury. Although activity is observed in the once-paralyzed diaphragm during and after CEES, this effect was not durable. It is possible that applying stimulation across several days or weeks could increase plasticity and long-term spontaneous muscle activity in the initially-paralyzed diaphragm. Methodologically, more plasticity occurs in the respiratory circuit in the C2 hemisection model that can be observed in the unanesthetized state compared to when anesthesia is a factor in the experimental set-up [170]. Future experiments should explore therapies that enhance plasticity in the awake, freely moving animal.

The author used CEES in awake animals beginning 3 days after C2 hemisection. There were several technical issues that affected outcomes, including stimulation delivery and its equipment and infection in

the animals. Technological advances in materials and engineering have allowed for broader use of small fabricated stimulation interfaces in research that can more closely mimic those used in the clinic. While expensive, these electrodes would provide better stimulation that can be replicated and better suited to explore subtle differences and electrode configurations best suited for respiratory neuromodulation. Additionally, the surgical technique to implant these electrodes would be simple, leading to more standardized surgeries.

Although the author used sterile technique, the surgical approach to secure the hardware to deliver stimulation led to infection and adverse outcomes. The technique of inserting screws into the skull and using dental cement to adhere the hardware in a stable place that can then be attached to connections for delivering stimulation and recording is well-known and widely used in many variations in neuroscience research. However, the author suggests securing the hardware below the base of the skull and between the two shoulder blades of the animal in future studies. This position is difficult for the animal to reach, and therefore would be less susceptible to interference. Additionally, this placement negates drilling into the skull, which is a traumatic injury to the animal and would ideally prevent the types of infections the author experienced on and around the skull.

Bench to Bedside

Diaphragm atrophy is a significant negative consequence of positive pressure mechanical ventilation and begins within several hours following use of mechanical ventilation [141, 179, 180]. Even without phrenic nerve damage, the diaphragm ceases to contract with use of positive pressure mechanical ventilation [140, 181]. This atrophy plays a role in failure to wean from mechanical ventilation, as the ability of the diaphragm to generate a higher maximum force compared to respiratory load predicts weaning success [182, 183]. However, both intermittent spontaneous breathes and phrenic nerve stimulation have shown to mitigate atrophy [181, 184, 185]. The author hypothesizes that, EES-induced respiratory circuit and muscle activity at the acute and sub-acute time points after injury would be more efficacious than starting in the chronic period years after spinal cord injury. This is in contrast to

rehabilitation improvements observed years after injury when EES is applied in conjunction with locomotor or upper extremity training after traumatic spinal cord injury [105, 150, 186, 187].

Continued experiments aimed at understanding the benefits and limitations of CEES as a clinical neuromodulation treatment for respiratory management or neurorehabilitation in cases of respiratory compromise is warranted. After rodents, larger mammals are required as a next step in the experimentation process to determine safety and feasibility. Although this therapy is FDA approved and has thus proven safe and feasible for chronic pain, larger mammals are likely still necessary to test safety of its implantation and use in the sub-acute time period after injury as this can be an unstable time for individuals with traumatic spinal cord injury with respiratory deficits. Another consideration in moving this therapy to clinical use is many clinical experiments aim to begin after at least one year out from the injury to allow for natural plasticity with rehabilitation that occurs within the first 12 months after injury [188-191]. Therefore, potential benefits of this treatment at the acute period (< 1 year) after injury, could be optimized and more safely executed with exploration in larger mammals.

For over a decade, research has shown that improvements are possible in lower and upper extremity function years after the initial spinal cord injury. Therefore, the safety and efficacy of the therapy when used in the chronic periods after injury has, to some extent been established [149, 186, 192, 193]. In fact, stabilization of blood pressure has been shown in the chronic period after spinal cord injury when EES is applied at the lumbar levels [194]. CEES in conjunction with respiratory rehabilitation should also be studied at the chronic time after injury. It is possible that, a population of individuals with cervical spinal cord injury would benefit even a year or more out following traumatic spinal cord injury. Well-controlled experiments using a cross-over design showing the effects of CEES applied after injury to improve respiratory outcomes would be able to elucidate some of these questions. Factors likely influencing these outcomes include extent of injury, age at time of injury, diet and physical fitness before and after injury, and psychological factors like motivation. Finally, working with a team of experienced respiratory therapists, pulmonologists, and nurses who understand the complications that arise in individuals with

spinal cord injury and the management of respiratory behaviors will enhance outcomes and the impact of future research.

References

1. Takahashi, K., et al., *Identification of the phrenic nucleus in the cat as studied by horseradish peroxidase bathing of the transected intrathoracal phrenic nerve.* Anat Anz, 1980. **148**(1): p. 49-54.
2. Goshgarian, H.G. and J.A. Rafols, *The phrenic nucleus of th albino rat: a correlative HRP and Golgi study.* J Comp Neurol, 1981. **201**(3): p. 441-56.
3. Mendelsohn, A.H., et al., *Cervical variations of the phrenic nerve.* The Laryngoscope, 2011. **121**(9): p. 1920-1923.
4. Ratnovsky, A., D. Elad, and P. Halpern, *Mechanics of respiratory muscles.* Respiratory Physiology & Neurobiology, 2008. **163**(1): p. 82-89.
5. Richter, D., D. Ballantyne, and J. Remmers, *How Is the Respiratory Rhythm Generated? A Model.* Physiology, 1986. **1**(3): p. 109-112.
6. Jenkin, S.E.M. and W.K. Milsom, *Chapter 8 - Expiration: Breathing's other face*, in *Progress in Brain Research*, G. Holstege, C.M. Beers, and H.H. Subramanian, Editors. 2014, Elsevier. p. 131-147.
7. Richter, D.W., *Generation and maintenance of the respiratory rhythm.* J Exp Biol, 1982. **100**: p. 93-107.
8. Todd, A.J., R.C. Spike, and E. Polgár, *A quantitative study of neurons which express neurokinin-1 or somatostatin sst2a receptor in rat spinal dorsal horn.* Neuroscience, 1998. **85**(2): p. 459-73.
9. Onimaru, H., A. Arata, and I. Homma, *Intrinsic burst generation of preinspiratory neurons in the medulla of brainstem-spinal cord preparations isolated from newborn rats.* Exp Brain Res, 1995. **106**(1): p. 57-68.
10. Feldman, J.L. and C.A. Del Negro, *Looking for inspiration: new perspectives on respiratory rhythm.* Nat Rev Neurosci, 2006. **7**(3): p. 232-42.
11. Martelli, D., D. Stanić, and M. Dutschmann, *The emerging role of the parabrachial complex in the generation of wakefulness drive and its implication for respiratory control.* Respir Physiol Neurobiol, 2013. **188**(3): p. 318-23.
12. Bautista, T.G. and M. Dutschmann, *Inhibition of the pontine Kölliker-Fuse nucleus abolishes eupneic inspiratory hypoglossal motor discharge in rat.* Neuroscience, 2014. **267**: p. 22-9.
13. Dutschmann, M. and H. Herbert, *The Kölliker-Fuse nucleus gates the postinspiratory phase of the respiratory cycle to control inspiratory off-switch and upper airway resistance in rat.* Eur J Neurosci, 2006. **24**(4): p. 1071-84.
14. Zuperku, E.J., et al., *Characteristics of breathing rate control mediated by a subregion within the pontine parabrachial complex.* Journal of Neurophysiology, 2017. **117**(3): p. 1030-1042.
15. Onimaru, H. and I. Homma, *A novel functional neuron group for respiratory rhythm generation in the ventral medulla.* J Neurosci, 2003. **23**(4): p. 1478-86.
16. Ikeda, K., et al., *A Phox2b BAC Transgenic Rat Line Useful for Understanding Respiratory Rhythm Generator Neural Circuitry.* PLoS One, 2015. **10**(7): p. e0132475.
17. Guyenet, P.G., et al., *Regulation of ventral surface chemoreceptors by the central respiratory pattern generator.* J Neurosci, 2005. **25**(39): p. 8938-47.
18. Kumar, N.N., et al., *PHYSIOLOGY. Regulation of breathing by CO_2 requires the proton-activated receptor GPR4 in retrotrapezoid nucleus neurons.* Science, 2015. **348**(6240): p. 1255-60.
19. Guyenet, P.G., R.L. Stornetta, and D.A. Bayliss, *Retrotrapezoid nucleus and central chemoreception.* The Journal of Physiology, 2008. **586**(8): p. 2043-2048.
20. Takakura, A.C., et al., *Peripheral chemoreceptor inputs to retrotrapezoid nucleus (RTN) CO2-sensitive neurons in rats.* J Physiol, 2006. **572**(Pt 2): p. 503-23.
21. Guyenet, P.G., et al., *Interdependent feedback regulation of breathing by the carotid bodies and the retrotrapezoid nucleus.* The Journal of Physiology, 2018. **596**(15): p. 3029-3042.

22. Miller, A.D., K. Ezure, and I. Suzuki, *Control of abdominal muscles by brain stem respiratory neurons in the cat.* J Neurophysiol, 1985. **54**(1): p. 155-67.
23. Dobbins, E.G. and J.L. Feldman, *Brainstem network controlling descending drive to phrenic motoneurons in rat.* Journal of Comparative Neurology, 1994. **347**(1): p. 64-86.
24. Tian, G.F., J.H. Peever, and J. Duffin, *Bötzinger-complex expiratory neurons monosynaptically inhibit phrenic motoneurons in the decerebrate rat.* Exp Brain Res, 1998. **122**(2): p. 149-56.
25. Smith, J.C., et al., *Pre-Bötzinger complex: a brainstem region that may generate respiratory rhythm in mammals.* Science, 1991. **254**(5032): p. 726-9.
26. Connelly, C.A., E.G. Dobbins, and J.L. Feldman, *Pre-Bötzinger complex in cats: respiratory neuronal discharge patterns.* Brain Res, 1992. **590**(1-2): p. 337-40.
27. Koizumi, H., et al., *Voltage-Dependent Rhythmogenic Property of Respiratory Pre-Bötzinger Complex Glutamatergic, Dbx1-Derived, and Somatostatin-Expressing Neuron Populations Revealed by Graded Optogenetic Inhibition.* eNeuro, 2016. **3**(3).
28. Cui, Y., et al., *Defining preBötzinger Complex Rhythm- and Pattern-Generating Neural Microcircuits In Vivo.* Neuron, 2016. **91**(3): p. 602-14.
29. Tan, W., et al., *Silencing preBötzinger complex somatostatin-expressing neurons induces persistent apnea in awake rat.* Nat Neurosci, 2008. **11**(5): p. 538-40.
30. Toporikova, N. and R.J. Butera, *Two types of independent bursting mechanisms in inspiratory neurons: an integrative model.* Journal of Computational Neuroscience, 2011. **30**(3): p. 515-528.
31. Rybak, I.A., et al., *Sodium Currents in Neurons From the Rostroventrolateral Medulla of the Rat.* Journal of Neurophysiology, 2003. **90**(3): p. 1635-1642.
32. Jasinski, P.E., et al., *Sodium and calcium mechanisms of rhythmic bursting in excitatory neural networks of the pre-Bötzinger complex: a computational modelling study.* Eur J Neurosci, 2013. **37**(2): p. 212-30.
33. Rybak, I.A., et al., *Rhythmic bursting in the pre-Bötzinger complex: mechanisms and models.* Prog Brain Res, 2014. **209**: p. 1-23.
34. Pace, R.W., et al., *Inspiratory bursts in the preBötzinger complex depend on a calcium-activated non-specific cation current linked to glutamate receptors in neonatal mice.* J Physiol, 2007. **582**(Pt 1): p. 113-25.
35. Del Negro, C.A., et al., *Sodium and calcium current-mediated pacemaker neurons and respiratory rhythm generation.* J Neurosci, 2005. **25**(2): p. 446-53.
36. Ellenberger, H.H. and J.L. Feldman, *Brainstem connections of the rostral ventral respiratory group of the rat.* Brain Research, 1990. **513**(1): p. 35-42.
37. Feldman, J.L., A.D. Loewy, and D.F. Speck, *Projections from the ventral respiratory group to phrenic and intercostal motoneurons in cat: an autoradiographic study.* J Neurosci, 1985. **5**(8): p. 1993-2000.
38. Tian, G.F. and J. Duffin, *The role of dorsal respiratory group neurons studied with cross-correlation in the decerebrate rat.* Exp Brain Res, 1998. **121**(1): p. 29-34.
39. Nakazono, Y. and M. Aoki, *Excitatory connections between upper cervical inspiratory neurons and phrenic motoneurons in cats.* J Appl Physiol (1985), 1994. **77**(2): p. 679-83.
40. Lipski, J. and J. Duffin, *An electrophysiological investigation of propriospinal inspiratory neurons in the upper cervical cord of the cat.* Experimental Brain Research, 1986. **61**(3): p. 625-637.
41. Kobayashi, S., et al., *Spontaneous respiratory rhythm generation in in vitro upper cervical slice preparations of neonatal mice.* J Physiol Sci, 2010. **60**(4): p. 303-7.
42. Hoskin, R.W., L.M. Fedorko, and J. Duffin, *Projections from upper cervical inspiratory neurons to thoracic and lumbar expiratory motor nuclei in the cat.* Experimental Neurology, 1988. **99**(3): p. 544-555.

43. Aoki, M., et al., *Supraspinal Descending Control of Propriospinal Respiratory Neurons in the Cat*, in *Respiratory Control: A Modeling Perspective*, G.D. Swanson, F.S. Grodins, and R.L. Hughson, Editors. 1989, Springer US: Boston, MA. p. 451-459.
44. Coglianese, C.J., C.N. Peiss, and R.D. Wurster, *Rhythmic phrenic nerve activity and respiratory activity in spinal dogs.* Respir Physiol, 1977. **29**(3): p. 247-54.
45. Mitchell, G.S., et al., *5-Hydroxytryptophan (5-HTP) augments spontaneous and evoked phrenic motoneuron discharge in spinalized rats.* Neuroscience Letters, 1992. **141**(1): p. 75-78.
46. Aoki, M., et al., *Generation of spontaneous respiratory rhythm in high spinal cats.* Brain Res, 1980. **202**(1): p. 51-63.
47. Gali, M.G.Z. and V. Marchenko, *Patterns of Phrenic Nerve Discharge after Complete High Cervical Spinal Cord Injury in the Decerebrate Rat.* Journal of Neurotrauma, 2016. **33**(12): p. 1115-1127.
48. Viala, D., C. Vidal, and E. Freton, *Coordinated rhythmic bursting in respiratory and locomotor muscle nerves in the spinal rabbit.* Neurosci Lett, 1979. **11**(2): p. 155-9.
49. Dhingra, R.R., et al., *Increasing Local Excitability of Brainstem Respiratory Nuclei Reveals a Distributed Network Underlying Respiratory Motor Pattern Formation.* Frontiers in Physiology, 2019. **10**(887).
50. Ikeda, K., et al., *The respiratory control mechanisms in the brainstem and spinal cord: integrative views of the neuroanatomy and neurophysiology.* J Physiol Sci, 2017. **67**(1): p. 45-62.
51. Ghali, M.G.Z., *Phrenic motoneurons: output elements of a highly organized intraspinal network.* J Neurophysiol, 2018. **119**(3): p. 1057-1070.
52. Marchenko, V., M.G. Ghali, and R.F. Rogers, *Motoneuron firing patterns underlying fast oscillations in phrenic nerve discharge in the rat.* J Neurophysiol, 2012. **108**(8): p. 2134-43.
53. Mitchell, R.A. and A.J. Berger, *Neural regulation of respiration.* Am Rev Respir Dis, 1975. **111**(2): p. 206-24.
54. Forster, H.V., P. Haouzi, and J.A. Dempsey, *Control of breathing during exercise.* Compr Physiol, 2012. **2**(1): p. 743-77.
55. Guyenet, P.G. and D.A. Bayliss, *Neural Control of Breathing and CO2 Homeostasis.* Neuron, 2015. **87**(5): p. 946-61.
56. Juvin, L., J. Simmers, and D. Morin, *Propriospinal Circuitry Underlying Interlimb Coordination in Mammalian Quadrupedal Locomotion.* The Journal of Neuroscience, 2005. **25**(25): p. 6025-6035.
57. McMurray, R.G. and S.W. Ahlborn, *Respiratory responses to running and walking at the same metabolic rate.* Respir Physiol, 1982. **47**(2): p. 257-65.
58. McMurray, R.G. and L.G. Smith, *Ventilatory responses when altering stride frequency at a constant oxygen uptake.* Respir Physiol, 1985. **62**(1): p. 117-24.
59. Jensen, V.N., W.J. Alilain, and S.A. Crone, *Role of Propriospinal Neurons in Control of Respiratory Muscles and Recovery of Breathing Following Injury.* Frontiers in Systems Neuroscience, 2020. **13**(84).
60. Zaki Ghali, M.G., G. Britz, and K.Z. Lee, *Pre-phrenic interneurons: Characterization and role in phrenic pattern formation and respiratory recovery following spinal cord injury.* Respir Physiol Neurobiol, 2019. **265**: p. 24-31.
61. Kirkwood, P.A., et al., *Respiratory interneurones in the thoracic spinal cord of the cat.* J Physiol, 1988. **395**: p. 161-92.
62. Saywell, S.A., et al., *Electrophysiological and Morphological Characterization of Propriospinal Interneurons in the Thoracic Spinal Cord.* Journal of Neurophysiology, 2011. **105**(2): p. 806-826.
63. Hilaire, G., M. Khatib, and R. Monteau, *Spontaneous respiratory activity of phrenic and intercostal Renshaw cells.* Neuroscience Letters, 1983. **43**(1): p. 97-101.

64. Hilaire, G., M. Khatib, and R. Monteau, *Central drive on Renshaw cells coupled with phrenic motoneurons.* Brain Research, 1986. **376**(1): p. 133-139.
65. Satkunendrarajah, K., et al., *Cervical excitatory neurons sustain breathing after spinal cord injury.* Nature, 2018. **562**(7727): p. 419-422.
66. Iizuka, M., et al., *Expressions of VGLUT1/2 in the inspiratory interneurons and GAD65/67 in the inspiratory Renshaw cells in the neonatal rat upper thoracic spinal cord.* IBRO Rep, 2018. **5**: p. 24-32.
67. Lane, M.A., et al., *Cervical prephrenic interneurons in the normal and lesioned spinal cord of the adult rat.* J Comp Neurol, 2008. **511**(5): p. 692-709.
68. Mulkey, D.K., et al., *Respiratory control by ventral surface chemoreceptor neurons in rats.* Nature neuroscience, 2004. **7**(12): p. 1360-1369.
69. Gonzalez, C., et al., *Carotid body chemoreceptors: from natural stimuli to sensory discharges.* Physiol Rev, 1994. **74**(4): p. 829-98.
70. SUSAN K. SCHULTZ, M.D. , Iowa City, Iowa, *Principles of Neural Science, 4th ed.* American Journal of Psychiatry, 2001. **158**(4): p. 662-662.
71. Bałkowiec, A., K. Kukuła, and P. Szulczyk, *Functional classification of afferent phrenic nerve fibres and diaphragmatic receptors in cats.* The Journal of physiology, 1995. **483 (Pt 3)**(Pt 3): p. 759-768.
72. Nair, J., et al., *Anatomy and physiology of phrenic afferent neurons.* J Neurophysiol, 2017. **118**(6): p. 2975-2990.
73. Yu, J. and M. Younes, *Powerful respiratory stimulation by thin muscle afferents.* Respiration Physiology, 1999. **117**(1): p. 1-12.
74. Nair, J., et al., *Histological identification of phrenic afferent projections to the spinal cord.* Respir Physiol Neurobiol, 2017. **236**: p. 57-68.
75. Davenport, P.W., R.L. Reep, and F.J. Thompson, *Phrenic nerve afferent activation of neurons in the cat SI cerebral cortex.* J Physiol, 2010. **588**(Pt 5): p. 873-86.
76. Zhang, W. and P.W. Davenport, *Activation of thalamic ventroposteriolateral neurons by phrenic nerve afferents in cats and rats.* J Appl Physiol (1985), 2003. **94**(1): p. 220-6.
77. Sauer, B. and N. Henderson, *Site-specific DNA recombination in mammalian cells by the Cre recombinase of bacteriophage P1.* Proc Natl Acad Sci U S A, 1988. **85**(14): p. 5166-70.
78. Sternberg, N. and D. Hamilton, *Bacteriophage P1 site-specific recombination. I. Recombination between loxP sites.* J Mol Biol, 1981. **150**(4): p. 467-86.
79. Nagel, G., et al., *Channelrhodopsin-2, a directly light-gated cation-selective membrane channel.* Proceedings of the National Academy of Sciences, 2003. **100**(24): p. 13940-13945.
80. Cregg, J.M., et al., *A Latent Propriospinal Network Can Restore Diaphragm Function after High Cervical Spinal Cord Injury.* Cell reports, 2017. **21**(3): p. 654-665.
81. Armbruster, B.N., et al., *Evolving the lock to fit the key to create a family of G protein-coupled receptors potently activated by an inert ligand.* Proceedings of the National Academy of Sciences, 2007. **104**(12): p. 5163-5168.
82. Alexander, G.M., et al., *Remote control of neuronal activity in transgenic mice expressing evolved G protein-coupled receptors.* Neuron, 2009. **63**(1): p. 27-39.
83. Merrill, E. and L. Fedorko, *Monosynaptic inhibition of phrenic motoneurons: a long descending projection from Botzinger neurons.* The Journal of Neuroscience, 1984. **4**(9): p. 2350-2353.
84. Parkis, M.A., et al., *Concurrent Inhibition and Excitation of Phrenic Motoneurons during Inspiration: Phase-Specific Control of Excitability.* The Journal of Neuroscience, 1999. **19**(6): p. 2368-2380.
85. Lee, K.-Z., *Phrenic motor outputs in response to bronchopulmonary C-fibre activation following chronic cervical spinal cord injury.* The Journal of Physiology, 2016. **594**(20): p. 6009-6024.

86. Kumar, K., R. Nath, and G.M. Wyant, *Treatment of chronic pain by epidural spinal cord stimulation: a 10-year experience.* Journal of Neurosurgery, 1991. **75**(3): p. 402.
87. Sdrulla, A.D., Y. Guan, and S.N. Raja, *Spinal Cord Stimulation: Clinical Efficacy and Potential Mechanisms.* Pain Practice, 2018. **18**(8): p. 1048-1067.
88. Grider, J.S., et al., *Effectiveness of Spinal Cord Stimulation in Chronic Spinal Pain: A Systematic Review.* Pain Physician, 2016. **19**(1): p. E33-54.
89. Darrow, D., et al., *Epidural Spinal Cord Stimulation Facilitates Immediate Restoration of Dormant Motor and Autonomic Supraspinal Pathways after Chronic Neurologically Complete Spinal Cord Injury.* J Neurotrauma, 2019. **36**(15): p. 2325-2336.
90. Taccola, G., et al., *And yet it moves: Recovery of volitional control after spinal cord injury.* Prog Neurobiol, 2018. **160**: p. 64-81.
91. Gerasimenko, Y.P., et al., *Spinal cord reflexes induced by epidural spinal cord stimulation in normal awake rats.* J Neurosci Methods, 2006. **157**(2): p. 253-63.
92. Huang, R., et al., *Modulation of respiratory output by cervical epidural stimulation in the anesthetized mouse.* J Appl Physiol (1985), 2016. **121**(6): p. 1272-1281.
93. Dobbins, E.G. and J.L. Feldman, *Brainstem network controlling descending drive to phrenic motoneurons in rat.* J Comp Neurol, 1994. **347**(1): p. 64-86.
94. Krashes, M.J., et al., *Rapid, reversible activation of AgRP neurons drives feeding behavior in mice.* The Journal of clinical investigation, 2011. **121**(4): p. 1424-1428.
95. Mondello, S.E., et al., *Optogenetic surface stimulation of the rat cervical spinal cord.* J Neurophysiol, 2018. **120**(2): p. 795-811.
96. Stornetta, R.L., et al., *A group of glutamatergic interneurons expressing high levels of both neurokinin-1 receptors and somatostatin identifies the region of the pre-Bötzinger complex.* J Comp Neurol, 2003. **455**(4): p. 499-512.
97. Smith, J.C., et al., *Brainstem respiratory networks: building blocks and microcircuits.* Trends Neurosci, 2013. **36**(3): p. 152-62.
98. Reynolds, S.C., et al., *Mitigation of Ventilator-induced Diaphragm Atrophy by Transvenous Phrenic Nerve Stimulation.* Am J Respir Crit Care Med, 2017. **195**(3): p. 339-348.
99. Le Pimpec-Barthes, F., et al., *Diaphragm pacing: the state of the art.* J Thorac Dis, 2016. **8**(Suppl 4): p. S376-86.
100. Bezdudnaya, T., M.A. Lane, and V. Marchenko, *Paced breathing and phrenic nerve responses evoked by epidural stimulation following complete high cervical spinal cord injury in rats.* Journal of Applied Physiology, 2018. **125**(3): p. 687-696.
101. Mercier, L.M., et al., *Intraspinal microstimulation and diaphragm activation after cervical spinal cord injury.* Journal of Neurophysiology, 2017. **117**(2): p. 767-776.
102. Kowalski, K.E., et al., *Diaphragm activation via high frequency spinal cord stimulation in a rodent model of spinal cord injury.* Experimental Neurology, 2013. **247**: p. 689-693.
103. Sunshine, M.D., et al., *Restoration of breathing after opioid overdose and spinal cord injury using temporal interference stimulation.* Communications Biology, 2021. **4**(1): p. 107.
104. Dimitrijevic, M.R., Y. Gerasimenko, and M.M. Pinter, *Evidence for a spinal central pattern generator in humans.* Ann N Y Acad Sci, 1998. **860**: p. 360-76.
105. Lavrov, I., et al., *Epidural Stimulation Induced Modulation of Spinal Locomotor Networks in Adult Spinal Rats.* The Journal of Neuroscience, 2008. **28**(23): p. 6022-6029.
106. Maeda, F., et al., *Modulation of corticospinal excitability by repetitive transcranial magnetic stimulation.* Clin Neurophysiol, 2000. **111**(5): p. 800-5.
107. Marlot, D., J.-M. Macron, and B. Duron, *Inhibitory and excitatory effects on respiration by phrenic nerve afferent stimulation in cats.* Respiration Physiology, 1987. **69**(3): p. 321-333.

108. Nair, J., et al., *Anatomy and physiology of phrenic afferent neurons.* Journal of Neurophysiology, 2017. **118**(6): p. 2975-2990.
109. Capogrosso, M., et al., *A Computational Model for Epidural Electrical Stimulation of Spinal Sensorimotor Circuits.* The Journal of Neuroscience, 2013. **33**(49): p. 19326.
110. Struijk, J.J., J. Holsheimer, and H.B. Boom, *Excitation of dorsal root fibers in spinal cord stimulation: a theoretical study.* IEEE Trans Biomed Eng, 1993. **40**(7): p. 632-9.
111. Holsheimer, J., *Which Neuronal Elements are Activated Directly by Spinal Cord Stimulation.* Neuromodulation, 2002. **5**(1): p. 25-31.
112. Malakhova, O.E. and P.W. Davenport, *c-Fos expression in the central nervous system elicited by phrenic nerve stimulation.* J Appl Physiol (1985), 2001. **90**(4): p. 1291-8.
113. Ward, M.E., et al., *Ventilatory effects of the interaction between phrenic and limb muscle afferents.* Respir Physiol, 1992. **88**(1-2): p. 63-76.
114. Goshgarian, H.G. and P.J. Roubal, *Origin and distribution of phrenic primary afferent nerve fibers in the spinal cord of the adult rat.* Exp Neurol, 1986. **92**(3): p. 624-38.
115. Duan, B., et al., *Identification of Spinal Circuits Transmitting and Gating Mechanical Pain.* Cell, 2014. **159**(6): p. 1417-1432.
116. Proudlock, F., R.C. Spike, and A.J. Todd, *Immunocytochemical study of somatostatin, neurotensin, GABA, and glycine in rat spinal dorsal horn.* Journal of Comparative Neurology, 1993. **327**(2): p. 289-297.
117. Gutierrez-Mecinas, M., et al., *A quantitative study of neurochemically defined excitatory interneuron populations in laminae I-III of the mouse spinal cord.* Mol Pain, 2016. **12**.
118. Xu, Y., et al., *Ontogeny of Excitatory Spinal Neurons Processing Distinct Somatic Sensory Modalities.* The Journal of Neuroscience, 2013. **33**(37): p. 14738-14748.
119. Chamessian, A., et al., *Transcriptional Profiling of Somatostatin Interneurons in the Spinal Dorsal Horn.* Scientific Reports, 2018. **8**(1): p. 6809.
120. Todd, A.J., *Neuronal circuitry for pain processing in the dorsal horn.* Nature reviews. Neuroscience, 2010. **11**(12): p. 823-836.
121. Willis, W.D., Jr., et al., *Projections from the marginal zone and deep dorsal horn to the ventrobasal nuclei of the primate thalamus.* Pain, 2001. **92**(1-2): p. 267-76.
122. Braz, J., et al., *Transmitting pain and itch messages: a contemporary view of the spinal cord circuits that generate gate control.* Neuron, 2014. **82**(3): p. 522-536.
123. Baba, H., et al., *Removal of GABAergic inhibition facilitates polysynaptic A fiber-mediated excitatory transmission to the superficial spinal dorsal horn.* Molecular and Cellular Neuroscience, 2003. **24**(3): p. 818-830.
124. Lu, Y., et al., *A feed-forward spinal cord glycinergic neural circuit gates mechanical allodynia.* J Clin Invest, 2013. **123**(9): p. 4050-62.
125. Bolser, D.C., et al., *Convergence of phrenic and cardiopulmonary spinal afferent information on cervical and thoracic spinothalamic tract neurons in the monkey: implications for referred pain from the diaphragm and heart.* J Neurophysiol, 1991. **65**(5): p. 1042-54.
126. Ikeda, K., et al., *The respiratory control mechanisms in the brainstem and spinal cord: integrative views of the neuroanatomy and neurophysiology.* The Journal of Physiological Sciences, 2017. **67**(1): p. 45-62.
127. Huckstepp, R.T.R., et al., *Role of parafacial nuclei in control of breathing in adult rats.* The Journal of neuroscience : the official journal of the Society for Neuroscience, 2015. **35**(3): p. 1052-1067.
128. Koshiya, N., et al., *Anatomical and functional pathways of rhythmogenic inspiratory premotor information flow originating in the pre-Bötzinger complex in the rat medulla.* Neuroscience, 2014. **268**: p. 194-211.

129. Marchenko, V. and R.F. Rogers, *GABAAergic and glycinergic inhibition in the phrenic nucleus organizes and couples fast oscillations in motor output.* J Neurophysiol, 2009. **101**(4): p. 2134-45.
130. Zaki Ghali, M.G., G. Britz, and K.-Z. Lee, *Pre-phrenic interneurons: Characterization and role in phrenic pattern formation and respiratory recovery following spinal cord injury.* Respiratory Physiology & Neurobiology, 2019. **265**: p. 24-31.
131. MacLaren, D.A., et al., *Clozapine N-Oxide Administration Produces Behavioral Effects in Long-Evans Rats: Implications for Designing DREADD Experiments.* eNeuro, 2016. **3**(5).
132. Goutaudier, R., et al., *DREADDs: The Power of the Lock, the Weakness of the Key. Favoring the Pursuit of Specific Conditions Rather than Specific Ligands.* eNeuro, 2019. **6**(5).
133. Martinez, V.K., et al., *Off-Target Effects of Clozapine-N-Oxide on the Chemosensory Reflex Are Masked by High Stress Levels.* Frontiers in Physiology, 2019. **10**(521).
134. Devivo, M.J., *Epidemiology of traumatic spinal cord injury: trends and future implications.* Spinal Cord, 2012. **50**(5): p. 365-72.
135. Galeiras Vázquez, R., et al., *Respiratory management in the patient with spinal cord injury.* Biomed Res Int, 2013. **2013**: p. 168757.
136. Berlowitz, D.J., B. Wadsworth, and J. Ross, *Respiratory problems and management in people with spinal cord injury.* Breathe (Sheff), 2016. **12**(4): p. 328-340.
137. Yang, L., et al., *Controlled mechanical ventilation leads to remodeling of the rat diaphragm.* Am J Respir Crit Care Med, 2002. **166**(8): p. 1135-40.
138. Madahar, P. and J.R. Beitler, *Emerging concepts in ventilation-induced lung injury.* F1000Res, 2020. **9**.
139. Smuder, A.J., et al., *Cervical spinal cord injury exacerbates ventilator-induced diaphragm dysfunction.* J Appl Physiol (1985), 2016. **120**(2): p. 166-77.
140. Powers, S.K., et al., *Mechanical ventilation results in progressive contractile dysfunction in the diaphragm.* J Appl Physiol (1985), 2002. **92**(5): p. 1851-8.
141. Levine, S., et al., *Rapid disuse atrophy of diaphragm fibers in mechanically ventilated humans.* N Engl J Med, 2008. **358**(13): p. 1327-35.
142. Son, B.C., et al., *Phrenic nerve stimulation for diaphragm pacing in a quadriplegic patient.* J Korean Neurosurg Soc, 2013. **54**(4): p. 359-62.
143. Naik, B.I., C. Lynch, and C.G. Durbin, *Variability in Mechanical Ventilation: What's All the Noise About?* Respiratory Care, 2015. **60**(8): p. 1203-1210.
144. Gonzalez-Rothi, E.J., et al., *High-frequency epidural stimulation across the respiratory cycle evokes phrenic short-term potentiation after incomplete cervical spinal cord injury.* Journal of Neurophysiology, 2017. **118**(4): p. 2344-2357.
145. DiMarco, A.F. and K.E. Kowalski, *High-frequency spinal cord stimulation of inspiratory muscles in dogs: a new method of inspiratory muscle pacing.* Journal of Applied Physiology, 2009. **107**(3): p. 662-669.
146. Sunshine, M.D., et al., *Respiratory resetting elicited by single pulse spinal stimulation.* Respiratory physiology & neurobiology, 2020. **274**: p. 103339-103339.
147. Sunshine, M.D., et al., *Intraspinal microstimulation for respiratory muscle activation.* Experimental Neurology, 2018. **302**: p. 93-103.
148. Epstein, L.J. and M. Palmieri, *Managing Chronic Pain With Spinal Cord Stimulation.* Mount Sinai Journal of Medicine: A Journal of Translational and Personalized Medicine, 2012. **79**(1): p. 123-132.
149. Angeli, C.A., et al., *Recovery of Over-Ground Walking after Chronic Motor Complete Spinal Cord Injury.* N Engl J Med, 2018. **379**(13): p. 1244-1250.

150. Ichiyama, R.M., et al., *Hindlimb stepping movements in complete spinal rats induced by epidural spinal cord stimulation.* Neuroscience Letters, 2005. **383**(3): p. 339-344.
151. Alam, M., et al., *Electrical neuromodulation of the cervical spinal cord facilitates forelimb skilled function recovery in spinal cord injured rats.* Experimental Neurology, 2017. **291**: p. 141-150.
152. Lu, D.C., et al., *Engaging Cervical Spinal Cord Networks to Reenable Volitional Control of Hand Function in Tetraplegic Patients.* Neurorehabil Neural Repair, 2016. **30**(10): p. 951-962.
153. Galer, E., et al., *Cervical epidural electrical stimulation increases respiratory activity in rats.* In Preparation, 2021.
154. Eldridge, F.L., D.E. Millhorn, and T. Waldrop, *Spinal inhibition of phrenic motoneurones by stimulation of afferents from leg muscle in the cat: blockade by strychnine.* J Physiol, 1987. **389**: p. 137-46.
155. Zimmer, M.B. and H.G. Goshgarian, *GABA, not glycine, mediates inhibition of latent respiratory motor pathways after spinal cord injury.* Exp Neurol, 2007. **203**(2): p. 493-501.
156. Marchenko, V., M.G. Ghali, and R.F. Rogers, *The role of spinal GABAergic circuits in the control of phrenic nerve motor output.* Am J Physiol Regul Integr Comp Physiol, 2015. **308**(11): p. R916-26.
157. Charsar, B.A., et al., *AAV2-BDNF promotes respiratory axon plasticity and recovery of diaphragm function following spinal cord injury.* Faseb j, 2019. **33**(12): p. 13775-13793.
158. Garraway, S.M. and J.R. Huie, *Spinal Plasticity and Behavior: BDNF-Induced Neuromodulation in Uninjured and Injured Spinal Cord.* Neural Plast, 2016. **2016**: p. 9857201.
159. Ghorbani, M., et al., *Impacts of epidural electrical stimulation on Wnt signaling, FAAH, and BDNF following thoracic spinal cord injury in rat.* Journal of Cellular Physiology, 2020. **235**(12): p. 9795-9805.
160. Farkas, S. and H. Ono, *Participation of NMDA and non-NMDA excitatory amino acid receptors in the mediation of spinal reflex potentials in rats: an in vivo study.* Br J Pharmacol, 1995. **114**(6): p. 1193-205.
161. Nelson, P.G., et al., *Mechanisms involved in activity-dependent synapse formation in mammalian central nervous system cell cultures.* J Neurobiol, 1990. **21**(1): p. 138-56.
162. Fields, R.D., C. Yu, and P.G. Nelson, *Calcium, network activity, and the role of NMDA channels in synaptic plasticity in vitro.* J Neurosci, 1991. **11**(1): p. 134-46.
163. Nantwi, K.D. and H.G. Goshgarian, *Theophylline-induced recovery in a hemidiaphragm paralyzed by hemisection in rats: contribution of adenosine receptors.* Neuropharmacology, 1998. **37**(1): p. 113-21.
164. Fuller, D.D., et al., *Synaptic Pathways to Phrenic Motoneurons Are Enhanced by Chronic Intermittent Hypoxia after Cervical Spinal Cord Injury.* The Journal of Neuroscience, 2003. **23**(7): p. 2993-3000.
165. Zhou, S.-Y., G.J. Basura, and H.G. Goshgarian, *Serotonin2 receptors mediate respiratory recovery after cervical spinal cord hemisection in adult rats.* Journal of Applied Physiology, 2001. **91**(6): p. 2665-2673.
166. Streeter, K.A., et al., *Intermittent Hypoxia Enhances Functional Connectivity of Midcervical Spinal Interneurons.* The Journal of Neuroscience, 2017. **37**(35): p. 8349-8362.
167. Streeter, K.A., et al., *Mid-cervical interneuron networks following high cervical spinal cord injury.* Respiratory Physiology & Neurobiology, 2020. **271**: p. 103305.
168. Alilain, W.J., et al., *Light-induced rescue of breathing after spinal cord injury.* J Neurosci, 2008. **28**(46): p. 11862-70.
169. Nantwi, K.D., et al., *Spontaneous Functional Recovery in a Paralyzed Hemidiaphragm Following Upper Cervical Spinal Cord Injury in Adult Rats.* Neurorehabilitation and Neural Repair, 1999. **13**(4): p. 225-234.

170. Bezdudnaya, T., et al., *Spontaneous respiratory plasticity following unilateral high cervical spinal cord injury in behaving rats.* Experimental Neurology, 2018. **305**: p. 56-65.
171. Dougherty, B.J., et al., *Contribution of the spontaneous crossed-phrenic phenomenon to inspiratory tidal volume in spontaneously breathing rats.* J Appl Physiol (1985), 2012. **112**(1): p. 96-105.
172. Goshgarian, H.G., *Invited Review: The crossed phrenic phenomenon: a model for plasticity in the respiratory pathways following spinal cord injury.* Journal of Applied Physiology, 2003. **94**(2): p. 795-810.
173. Dale-Nagle, E.A., et al., *Spinal plasticity following intermittent hypoxia: implications for spinal injury.* Ann N Y Acad Sci, 2010. **1198**: p. 252-9.
174. Burns, S.P., et al., *Recovery of ambulation in motor-incomplete tetraplegia.* Arch Phys Med Rehabil, 1997. **78**(11): p. 1169-72.
175. Bradbury, E.J. and S.B. McMahon, *Spinal cord repair strategies: why do they work?* Nat Rev Neurosci, 2006. **7**(8): p. 644-53.
176. Herrera, D.G. and H.A. Robertson, *Activation of c-fos in the brain.* Prog Neurobiol, 1996. **50**(2-3): p. 83-107.
177. Card, J., et al., *Neurotropic properties of pseudorabies virus: uptake and transneuronal passage in the rat central nervous system.* The Journal of Neuroscience, 1990. **10**(6): p. 1974-1994.
178. Rinaman, L., J. Card, and L. Enquist, *Spatiotemporal responses of astrocytes, ramified microglia, and brain macrophages to central neuronal infection with pseudorabies virus.* The Journal of Neuroscience, 1993. **13**(2): p. 685-702.
179. Jaber, S., et al., *Rapidly progressive diaphragmatic weakness and injury during mechanical ventilation in humans.* Am J Respir Crit Care Med, 2011. **183**(3): p. 364-71.
180. Goligher, E.C., et al., *Evolution of Diaphragm Thickness during Mechanical Ventilation. Impact of Inspiratory Effort.* American Journal of Respiratory and Critical Care Medicine, 2015. **192**(9): p. 1080-1088.
181. Sassoon, C.S., E. Zhu, and V.J. Caiozzo, *Assist-control mechanical ventilation attenuates ventilator-induced diaphragmatic dysfunction.* Am J Respir Crit Care Med, 2004. **170**(6): p. 626-32.
182. Carlucci, A., et al., *Determinants of weaning success in patients with prolonged mechanical ventilation.* Crit Care, 2009. **13**(3): p. R97.
183. Goligher, E.C., et al., *Mechanical Ventilation–induced Diaphragm Atrophy Strongly Impacts Clinical Outcomes.* American Journal of Respiratory and Critical Care Medicine, 2018. **197**(2): p. 204-213.
184. Gayan-Ramirez, G., et al., *Intermittent spontaneous breathing protects the rat diaphragm from mechanical ventilation effects.* Crit Care Med, 2005. **33**(12): p. 2804-9.
185. Yang, M., et al., *Phrenic nerve stimulation protects against mechanical ventilation-induced diaphragm dysfunction in rats.* Muscle & Nerve, 2013. **48**(6): p. 958-962.
186. Harkema, S., et al., *Effect of epidural stimulation of the lumbosacral spinal cord on voluntary movement, standing, and assisted stepping after motor complete paraplegia: a case study.* Lancet, 2011. **377**(9781): p. 1938-47.
187. Lu, D.C., et al., *Engaging Cervical Spinal Cord Networks to Reenable Volitional Control of Hand Function in Tetraplegic Patients.* Neurorehabilitation and Neural Repair, 2016. **30**(10): p. 951-962.
188. Herzer, K.R., et al., *Association Between Time to Rehabilitation and Outcomes After Traumatic Spinal Cord Injury.* Arch Phys Med Rehabil, 2016. **97**(10): p. 1620-1627.e4.
189. Fouad, K. and A. Tse, *Adaptive changes in the injured spinal cord and their role in promoting functional recovery.* Neurol Res, 2008. **30**(1): p. 17-27.

190. Dietz, V. and G. Colombo, *Recovery from spinal cord injury--underlying mechanisms and efficacy of rehabilitation.* Acta Neurochir Suppl, 2004. **89**: p. 95-100.
191. Calancie, B., M.R. Molano, and J.G. Broton, *Interlimb reflexes and synaptic plasticity become evident months after human spinal cord injury.* Brain, 2002. **125**(Pt 5): p. 1150-61.
192. Gill, M.L., et al., *Neuromodulation of lumbosacral spinal networks enables independent stepping after complete paraplegia.* Nat Med, 2018. **24**(11): p. 1677-1682.
193. Wagner, F.B., et al., *Targeted neurotechnology restores walking in humans with spinal cord injury.* Nature, 2018. **563**(7729): p. 65-71.
194. Harkema, S.J., et al., *Normalization of Blood Pressure With Spinal Cord Epidural Stimulation After Severe Spinal Cord Injury.* Frontiers in Human Neuroscience, 2018. **12**: p. 83.